ÖAW AUSTRIAN ACADEMY OF SCIENCES

Johann Radon Institute for
Computational and Applied Mathematics
Austrian Academy of Sciences (ÖAW)

RICAM
JOHANN · RADON · INSTITUTE
FOR COMPUTATIONAL AND APPLIED MATHEMATICS

A family of C^1 quadrilateral finite elements

M. Kapl, G. Sangalli, T. Takacs

RICAM-Report 2020-20

A FAMILY OF C^1 QUADRILATERAL FINITE ELEMENTS

MARIO KAPL, GIANCARLO SANGALLI, AND THOMAS TAKACS

Abstract. We present a novel family of C^1 quadrilateral finite elements, which define global C^1 spaces over a quadrilateral mesh with possibly extraordinary vertices (i.e. vertices with a valency different to four). The elements generalize the construction by Brenner and Sung [8], which is based on polynomial elements of tensor-product degree $p \geq 6$. Thus, we call the family of C^1 finite elements *Brenner-Sung quadrilaterals*. The construction is extended to all degrees $p \geq 3$. Note that the proposed quadrilateral elements possess similar degrees of freedom as the classical Argyris triangles [1]. Just as the Argyris triangle, the Brenner-Sung quadrilateral is additionally C^2 at the vertices. The construction of the C^1 quadrilateral is given for bivariate polynomials of bi-degree (p, p) with $p \geq 5$, and can be extended to the lower polynomial degrees $p = 3$ and $p = 4$ by employing a splitting into 3×3 or 2×2, respectively, polynomial pieces. These piecewise polynomial functions can be represented as B-splines.

We prove that the proposed quadrilateral elements and their resulting global C^1 spaces reproduce polynomials of total degree p. Moreover, we show that the space provides optimal approximation order for errors in Sobolev norms as well as in L^∞. Due to the interpolation properties, the error bounds are local on each element. In addition, we describe the construction of a simple, local basis of the Brenner-Sung quadrilateral, and give for several particular cases explicit formulas for the Bézier or B-spline coeffients of the basis functions. Numerical experiments by solving the biharmonic equation over several quadrilateral meshes demonstrate the potential of the C^1 quadrilateral finite element for the numerical analysis of fourth order problems. Moreover, some further numerical tests also indicate that (for $p = 5$) the Brenner-Sung quadrilateral performs comparable or in general even better than the Argyris triangle with respect to the number of degrees of freedom.

1. Introduction

Using a standard Galerkin approach for the numerical analysis of high order problems, globally smooth function spaces are needed. E.g., for solving fourth order partial differential equations (PDEs) via the finite element method (FEM), C^1 finite element spaces are required, which in general using polynomials of higher degree. In the case of triangular meshes, two popular and well-known examples are the Argyris element [1] and the Bell element [3]. Both elements require polynomials of degree $p \geq 5$, and are additionally C^2 at the vertices. While the normal derivative along an edge is of degree $p - 1$ for the Argyris element, its degree reduces to $p - 2$ for the Bell element. This leads for instance in case of polynomial degree $p = 5$ to the fact that the Argyris triangular space possesses six degrees of freedom for each vertex and one degree of freedom for each edge, while the Bell triangular space just has six degrees of freedom for each vertex and no additional degrees of freedom for

Date: March 12, 2020.

2010 *Mathematics Subject Classification.* Primary 65N30, secondary 65D07.

the edges. For more details on the Argyris and Bell triangular element as well as on other C^1 triangular finite elements, we refer to the books [7, 12]. A possiblity to get C^1 finite element spaces of lower polynomial degree is to use splines over triangular meshes. However, this requires in general special splits of the triangles such as the Clough-Tocher or Powell-Sabin 6- or 12-splits, see e.g. [34].

The design of C^1 finite elements over quadrilateral meshes is in general more challenging compared to the case of triangular meshes, in particular with respect to the selection of the degrees of freedom. Examples of C^1 quadrilateral elements are [4, 6, 8, 35]. The Bogner-Fox-Schmit element [6] is a simple bivariate Hermite type C^1 construction which works for low polynomial degrees such as $p = 3$, but is limited to tensor-product meshes. In contrast, the C^1 elements [4, 8, 35] are applicable to more general quadrilateral meshes with possibly extraordinary vertices (i.e. vertices with a patch valency different to four), but require a polynomial degree $p \geq 6$ in case of [8] and a polynomial degree $p \geq 5$ (for some specific settings just $p = 4$) in case of [4, 35]. The degrees of freedom for the finite element space [8] are selected similar to the Argyris [1] and Bell triangular finite element space [3] by enforcing additionally C^2-continuity at the vertices, which we also follow in our approach. In contrast, the functions in [4, 35] are just C^1 at the vertices and the degrees of freedom are defined by means of the concept of minimal determining sets (cf. [34]), which is a common strategy for the construction of C^1 splines over triangular meshes, see also [34]. A different but related problem is the construction of C^1 function spaces over general quadrilateral meshes for the design of surfaces, such as in [18, 40, 41, 44]. The methods are based on the concept of geometric continuity [42], which is a well-known tool in computer aided geometric design for generating smooth complex surfaces.

An alternative to FEM is the use of isogeometric analysis (IgA), which was introduced in [21], and employs the same spline function space for describing the physical domain of interest and for representing the solution of the considered PDE, see e.g. [2, 14, 21] for more details. In case of a single patch geometry, this allows a simple and fast discretization of high order PDEs [48], such as the Kirchhoff-Love shells, e.g. [33, 32], the Navier-Stokes-Korteweg equation, e.g. [17], problems of strain gradient elasticity, e.g. [15, 39], or the Cahn-Hilliard equation, e.g. [16], by just using the higher regularity of the splines. In case of multi-patch geometries with possibly extraordinary vertices, that is, in case of unstructured quadrilateral meshes, the design of smooth spline spaces is challenging and is the topic of current research. In [9, 45, 47], different approaches for the construction of smooth spline functions of degree p are presented, which are C^s $(1 \leq s \leq p-1)$ everywhere, except in the vicinity of an extraordinary vertex, where they are just C^0.

The construction of globally C^1 spline functions over unstructured quadrilateral meshes relies on the equivalence relation that an isoparametric function is C^1 if and only if it possesses a graph surface which is geometric continuous of order 1 (i.e. C^1 after possible reparameterizations of the graph surface patches), cf. [13, 19, 28]. Depending on the used type of parameterizations for the single patches of the given unstructured quadrilateral mesh, different techniques for the design of a C^1 spline space over this mesh have been developed. Possible examples in the case of planar, unstructured quadrilateral meshes are to use C^1 multi-patch parameterizations with a singularity at an extraordinary vertex, e.g. [38, 49], multi-patch parameterizations which are C^1 except in the vicinity of an extraordinary vertex, e.g. [29, 30, 31, 37],

or multi-patch parameterizations which have to be just C^0 at all interfaces, e.g. [5, 10, 11, 13, 23, 24, 25, 27, 28, 36]. For more details about existing C^1 constructions for unstructured quadrilateral meshes, we refer to the recent survey article [26].

In this work, we present the design of a novel family of C^1 quadrilateral finite elements, whose resulting C^1 space possesses similar degress of freedom as the classical Argyris triangle space [1]. The construction extends the C^1 element developed in [8] and is therefore referred to as the Brenner-Sung quadrilateral. The construction of the C^1 quadrilateral finite element space is related to the work in [27], where a C^1 isogeometric spline space for a particular class of planar, unstructured quadrilateral meshes was generated. Like for the Argyris triangle, the Brenner-Sung quadrilateral is additionally C^2 at the vertices, and can be easily constructed via a simple, local interpolation problem by employing bivariate polynomials of bi-degree (p, p) with $p \geq 5$. An advantage of our C^1 quadrilateral construction over the triangular one is the simpler extension to the lower polynomial degrees $p = 3$ and $p = 4$ by just using tensor-product spline macro-elements without the need of special splits for the mesh elements.

While in [27] the optimal approximation properties of the C^1 isogeometric spline space is just numerically shown, in this work the optimal approximation order of the Brenner-Sung quadrilateral space is proven in terms of local and global error estimates in L^∞ as well as in L^2, H^1 and H^2 Sobolev norms. A further extension to [27] is that for some particular cases the Bézier or spline coefficients of the basis functions are explicitly given by simple formulas. Several numerical tests of solving the biharmonic equation also show the potential of the Brenner-Sung quadrilateral space for the numerical analysis of fourth order PDEs.

The outline of this paper is as follows. Section 2 introduces the quadrilateral mesh which will be used throughout the paper. In Section 3, the construction of the Brenner-Sung quadrilateral is described, which is first done for the case of bi-quintic polynomials, for degrees $p \geq 6$ as in [8], and then for a first extension to spline elements, which allow the use of the lower polynomial degrees $p = 3$ and $p = 4$, too. A more general extension to C^1 quadrilateral spline elements is described later in Section 5. Section 3 also discusses the connection of the Brenner-Sung quadrilateral with two well-known triangular finite elements, namely with the Argyris triangle [1] and with the Bell triangle [3], and studies several properties of the Brenner-Sung quadrilateral space such as polynomial reproduction and error estimates in Sobolev norms. Then, Sections 4 and 5 describe the design of local basis functions of the Brenner-Sung quadrilateral space for the case of polynomials and its extension for the case of splines, respectively, and state for some particular cases explicitly given formulas for the Bézier and spline coefficients of the basis functions. The possible extension of the Brenner-Sung quadrilateral to an isoparametric/isogeometric element is briefly discussed in Section 6. Finally, we present in Section 7 numerical examples of solving the biharmonic equation on different quadrilateral meshes, and conclude the paper in Section 8.

2. The physical domain and mesh

In this paper we consider planar domains that allow meshing by quadrilaterals. Note that a generalization to domains with curved boundaries is possible with some additional care. We refer the reader to [4, 25], where such discretizations were developed.

2.1. **The physical domain.** We assume the physical domain to be an open, planar, connected region $\Omega \subset \mathbb{R}^2$, which may be simply connected or it may have holes. The domain must allow a quadrangulation, as defined below. This is the case if the boundary (including all inner boundaries) is piecewise linear. The coordinates in physical space are given as (x, y) and we denote the derivatives of functions on Ω in x- and in y-direction with ∂_x and ∂_y, respectively.

2.2. **The quadrilateral mesh and its objects.** We consider a quadrilateral mesh as a tuple

$$\mathcal{M} = (\mathcal{Q}, \mathcal{E}, \mathcal{V}),$$

consisting of a set of quadrilaterals $\mathcal{Q}$, edges $\mathcal{E}$ and vertices $\mathcal{V}$ satisfying the following properties.

- Each vertex $v \in \mathcal{V}$ is a point in the plane, i.e., for all $v \in \mathcal{V}$ we have $v \in \mathbb{R}^2$.
- For each edge $\varepsilon \in \mathcal{E}$ there exist two vertices $v_1, v_2 \in \mathcal{V}$ such that

$$\varepsilon = \{(1-s)\, v_1 + s\, v_2 : s \in]0,1[\}.$$

- For each quadrilateral $Q \in \mathcal{Q}$ there exist four vertices $v_1, \dots, v_4 \in \mathcal{V}$ and four edges $\varepsilon_1, \dots, \varepsilon_4 \in \mathcal{E}$, with edge ε_i connecting v_i with v_{i+1} (modulo 4), given in counter-clockwise order, and a regular, bilinear parametrization $\mathbf{F}_Q : \widehat{Q} \to \overline{Q}$, with $\widehat{Q} = [0,1]^2$, such that

$$\mathbf{F}_Q(\xi_1, \xi_2) = (1-\xi_1)(1-\xi_2)\, v_1 + \xi_1(1-\xi_2)\, v_2 + \xi_1\xi_2\, v_3 + (1-\xi_1)\xi_2\, v_4.$$

  See Fig. 1 for a visualization.

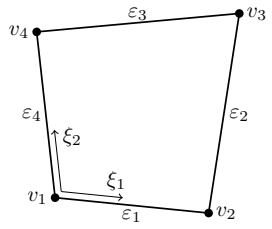

FIGURE 1. Vertices, edges and local coordinates for one quadrilateral Q.

All quadrilaterals are assumed to be shape regular, i.e., the parametrizations satisfy

$$0 < \rho \leq \frac{\det(\nabla \mathbf{F}_Q(\xi_1, \xi_2))}{(h_Q)^2} \leq 1 \tag{2.1}$$

with a given shape regularity parameter ρ. Here $h_Q = \max_{1 \leq i \leq 4}(h_{\varepsilon_i})$, where h_{ε_i} denotes the length of the edge ε_i. Note that the right inequality in (2.1) is always satisfied, since the Jacobian determinant is a measure for the area of the patch. From this shape regularity condition it immediately follows, that $h_Q = \max_{1 \leq i \leq 4}(h_{\varepsilon_i}) \leq \frac{1}{\sqrt{\rho}} \min_{1 \leq i \leq 4}(h_{\varepsilon_i})$.

As a custom, we define all quadrilaterals to be open and all edges not to include the vertices. Thus, we can introduce the following definition of a valid quadrangulation.

Definition 2.1. We say that the mesh $\mathcal{M}$ is a (valid) *quadrangulation* of the physical domain Ω, if

$$\overline{\Omega} = \bigcup_{Q \in \mathcal{Q}} \overline{Q}$$

and all intersections of different mesh elements are empty, i.e., for all $X, X' \in \mathcal{Q} \cup \mathcal{E} \cup \mathcal{V}$, with $X \neq X'$, we have $X \cap X' = \emptyset$.

3. The C^1 quadrilateral elements

In the following we define a piecewise polynomial C^1 space over the domain of interest Ω, given a quadrilateral mesh $\mathcal{M}$ as a quadrangulation of Ω. In our presentation we loosely follow the style of [7, 12]. The Brenner-Sung space of degree $p \geq 5$ is bi-quintic on each quadrilateral element, where all normal derivatives across interfaces are polynomials of degree $p-1$. For $p = 5$ the degrees of freedom are given as C^2-data at the vertices, normal derivatives at the edge midpoints, as well as interior point evaluations. This is in accordance with the degrees of freedom of the Argyris triangle, see [1]. Moreover, one can define piecewise polynomial spaces of degree $p \in \{3, 4\}$, where the quadrilaterals have to be considered as macro-elements and subdivided further. This is explained in more detail in Subsections 3.4 and 5.1.

We denote with $\mathbb{P}^{(p,p)}$ the space of bivariate polynomials of bi-degree (p, p) and with $\mathbb{P}^p$ the space of polynomials of total degree p, either uni- or bivariate, depending on context.

In the next subsections we introduce the local spaces and degrees of freedom corresponding to a single quadrilateral Q. To do this, we need the following notation.

Definition 3.1 (Pre-images of points and edges)**.** For every point $v \in \mathbb{R}^2$, with $v \in \overline{Q}$, we define $\hat{v}$ as the pre-image of v under $\mathbf{F}_Q$, i.e., $\hat{v} = \mathbf{F}_Q^{-1}(v)$. Analogously, we define $\hat{\varepsilon} = \mathbf{F}_Q^{-1}(\varepsilon)$ for $\varepsilon \in \mathcal{E}$ with $\varepsilon \subset \overline{Q}$. In Fig. 1 we have, e.g., $\hat{v}_1 = (0, 0)^T$.

One set of degrees of freedom is the normal derivative at the edge midpoint, where we use the following notation. For every edge $\varepsilon \in \mathcal{E}$ between vertices v_1 and v_2, let $m_\varepsilon = \frac{1}{2}v_1 + \frac{1}{2}v_2$ be the edge midpoint. Moreover, let $\mathbf{n}_\varepsilon$ be its normal vector and $\partial_{\mathbf{n}_\varepsilon}$ be the normal derivative of a function defined on Ω across the edge ε. Here we assume that the direction of the normal is fixed for every edge of the mesh $\mathcal{M}$.

3.1. The local space and degrees of freedom for degree $p = 5$.

Given a quadrilateral $Q \in \mathcal{Q}$ we define the local function space and the local degrees of freedom as follows.

Definition 3.2 (Brenner-Sung quadrilateral for $p = 5$)**.** Given a quadrilateral Q with vertices v_1, v_2, v_3 and v_4 and edges ε_1, ε_2, ε_3 and ε_4 we define the Brenner-Sung quadrilateral of degree $p = 5$ as (Q, P_Q^5, Λ_Q^5), with

(3.1)
$$P_Q^5 = \left\{ \varphi : \overline{Q} \to \mathbb{R}, \text{ with } (\varphi \circ \mathbf{F}_Q) \in \mathbb{P}^{(5,5)}, (\partial_{\mathbf{n}_{\varepsilon_i}} \varphi \circ \mathbf{F}_Q)|_{\hat{\varepsilon}_i} \in \mathbb{P}^4, \ 1 \leq i \leq 4 \right\}$$

and

(3.2)
$$\begin{aligned} \Lambda_Q^5 &= \Lambda_{0,Q} \cup \Lambda_{1,Q} \cup \Lambda_{2,Q}^5, \text{ with} \\ \Lambda_{0,Q} &= \{\varphi(v_i), \partial_x\varphi(v_i), \partial_y\varphi(v_i), \partial_x\partial_x\varphi(v_i), \partial_x\partial_y\varphi(v_i), \partial_y\partial_y\varphi(v_i), \ 1 \leq i \leq 4\}, \\ \Lambda_{1,Q} &= \left\{\partial_{\mathbf{n}_{\varepsilon_i}}\varphi(m_{\varepsilon_i}), \ 1 \leq i \leq 4\right\}, \\ \Lambda_{2,Q}^5 &= \left\{\varphi(x), \ x \in \mathcal{F}_Q^5\right\}. \end{aligned}$$

The set of face points is given as

$$\mathcal{F}_Q^5 = \left\{ \mathbf{F}_Q\left(\eta_1, \eta_2\right),\ \eta_1, \eta_2 \in \left\{ \frac{2}{5}, \frac{3}{5} \right\} \right\}.$$

See Fig. 2 for a visualization of the local degrees of freedom of the Brenner-Sung quadrilateral.

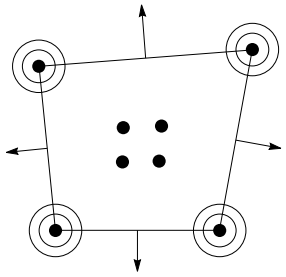

FIGURE 2. The Brenner-Sung quadrilateral for $p = 5$, visualizing the degrees of freedom Λ_Q^5.

A generalization of this element to higher degrees $p \geq 6$ can be found in [8] as well as in Subsection 5.1, where all polynomial cases are covered by $k = 1$. We explicitly formulate the polynomial case in the following subsection.

3.2. **The local space and degrees of freedom for degree $p \geq 6$.** Given a quadrilateral $Q \in \mathcal{Q}$ we define the local function space and the local degrees of freedom for $p \geq 6$ as follows.

Definition 3.3 (Brenner-Sung quadrilateral [8])**.** Given a quadrilateral Q with vertices v_1, v_2, v_3 and v_4 and edges ε_1, ε_2, ε_3 and ε_4 we define the Brenner-Sung quadrilateral of degree $p \geq 6$ as (Q, P_Q^p, Λ_Q^p), with

(3.3)
$$P_Q^p = \left\{ \varphi : \overline{Q} \to \mathbb{R},\ \text{with } (\varphi \circ \mathbf{F}_Q) \in \mathbb{P}^{(p,p)}, (\partial_{\mathbf{n}_{\varepsilon_i}} \varphi \circ \mathbf{F}_Q)|_{\hat{\varepsilon}_i} \in \mathbb{P}^{p-1},\ 1 \leq i \leq 4 \right\}$$

and

(3.4)
$$\begin{aligned}
\Lambda_Q^p &= \Lambda_{0,Q} \cup \Lambda_{1,Q}^p \cup \Lambda_{2,Q}^p,\ \text{with} \\
\Lambda_{0,Q} &= \{\varphi(v_i), \partial_x\varphi(v_i), \partial_y\varphi(v_i), \partial_x\partial_x\varphi(v_i), \partial_x\partial_y\varphi(v_i), \partial_y\partial_y\varphi(v_i),\ 1 \leq i \leq 4\}, \\
\Lambda_{1,Q}^* &= \left\{ \varphi(\mathbf{F}_{\varepsilon_i}(\tfrac{j}{p})),\ \ \text{for } 1 \leq i \leq 4,\ 3 \leq j \leq p-3 \right\} \\
&\qquad \cup \left\{ \partial_{\mathbf{n}_{\varepsilon_i}} \varphi(\mathbf{F}_{\varepsilon_i}(\tfrac{j}{p-1})),\ \ \text{for } 1 \leq i \leq 4,\ 2 \leq j \leq p-3 \right\}, \\
\Lambda_{2,Q}^p &= \left\{ \varphi(x),\ x \in \mathcal{F}_Q^p \right\}.
\end{aligned}$$

Here $\mathbf{F}_{\varepsilon_i} = \mathbf{F}_Q|_{\varepsilon_i}$, and the set of face points is given as

$$\mathcal{F}_Q^p = \left\{ \mathbf{F}_Q\left(\eta_1, \eta_2\right),\ \eta_1, \eta_2 \in \left\{ \frac{2}{p}, \ldots, \frac{p-2}{p} \right\} \right\}.$$

As one can easily see, Definition 3.3 covers also the case of Definition 3.2. Obviously, we have the following.

Lemma 3.4. *Any function $\varphi \in P_Q^p$, for $p \geq 5$, is completely determined by the degrees of freedom Λ_Q^p. The space satisfies* $\dim(P_Q^p) = |\Lambda_Q^p| = (p+1)^2 - 4$.

Proof. The dimension of P_Q^p is given by $\dim(\mathbb{P}^{(p,p)}) = (p+1)^2$, reduced by the number of independent constraints $(\partial_{\mathbf{n}_{\varepsilon_i}} \varphi \circ \mathbf{F}_Q)|_{\hat{\varepsilon}_i} \in \mathbb{P}^{p-1}$, which are one per edge, i.e., four. We also have $|\Lambda_Q^p| = 4 \times 6 + 4 \times (p-5) + 4 \times (p-4) + (p-3)^2$, where all functionals in Λ_Q^p are independent. Thus, the statement follows. □

3.3. **Connection to the Argyris and Bell triangles.** We have already observed the similarity with the Argyris triangle. Let us recall the definition of the Argyris triangle for $p = 5$ as given in [1, 12].

Definition 3.5 (Argyris triangle for $p = 5$)**.** Given a triangle T with vertices v_1, v_2 and v_3 and edges ε_1, ε_2 and ε_3 we define the Argyris triangle as (T, P_T, Λ_T), with $P_T = \mathbb{P}^5$ and $\Lambda_T = \Lambda_{0,T} \cup \Lambda_{1,T}$, with

$$\Lambda_{0,T} = \{\varphi(v_i), \partial_x\varphi(v_i), \partial_y\varphi(v_i), \partial_x\partial_x\varphi(v_i), \partial_x\partial_y\varphi(v_i), \partial_y\partial_y\varphi(v_i),\ 1 \leq i \leq 3\},$$
$$\Lambda_{1,T} = \left\{\partial_{\mathbf{n}_{\varepsilon_i}}\varphi(m_{\varepsilon_i}),\ 1 \leq i \leq 3\right\}.$$

Hence, the degrees of freedom for the Brenner-Sung quadrilateral and Argyris triangle are the same, except for the additional point evaluations at face points in the quadrilateral case. In addition, the traces as well as normal derivatives along edges are the same in both elements, i.e., for $p = 5$ traces are quintic polynomials and normal derivatives are quartic polynomials. The degrees of freedom for the Argyris triangle are visualized in Figure 3 (left).

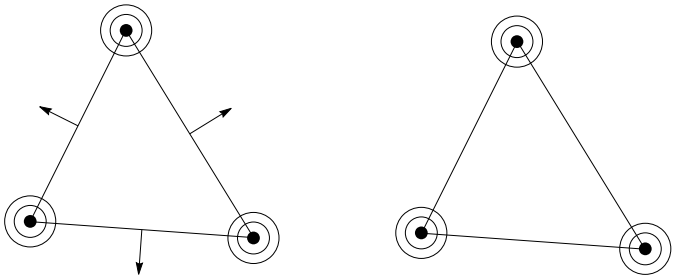

FIGURE 3. The Argyris triangle (left) and Bell triangle (right), visualizing Λ_T^A and Λ_T^B, respectively.

In addition, the condition that the normal derivative along an edge is of degree 4, is similar to the condition on the Bell triangular element [3], a quintic element, where normal derivatives are assumed to be polynomials of degree 3, thus eliminating the normal derivative degrees of freedom and resulting in 18 degrees of freedom per triangle.

Definition 3.6 (Bell triangle for $p = 5$)**.** Given a triangle T with vertices v_1, v_2 and v_3 and edges ε_1, ε_2 and ε_3 we define the Bell triangle as (T, P_T^B, Λ_T^B), with

$$P_T^B = \left\{\varphi : \overline{T} \to \mathbb{R},\ \text{with } \varphi \in \mathbb{P}^5,\ \partial_{\mathbf{n}_{\varepsilon_i}}\varphi|_{\varepsilon_i} \in \mathbb{P}^3,\ 1 \leq i \leq 3\right\} \tag{3.5}$$

and $\Lambda_T^B = \Lambda_{0,T}$.

The degrees of freedom for the Bell triangle are visualized in Figure 3 (right). Both triangle elements possess variants of higher degree, see [1, 3, 12, 34]. For triangular elements, constructions of smooth spaces for lower degrees are usually based on special splits, such as the Clough-Tocher or Powell-Sabin 6- or 12-splits. Unlike the triangular case, in the quadrilateral case variants of lower degree are relatively straightforward and follow from the spline constructions developed in [27].

3.4. **The local space and degrees of freedom for lower degrees $p \in \{3,4\}$.** In the following we extend the construction on quadrilaterals to lower degrees $p = 3$ and $p = 4$ using a split into sub-elements, as in Fig. 4. We assume that the parameter domain $\widehat{Q}$ is split into sub-elements $\hat{q} \in s_k(\widehat{Q})$, with

$$s_k(\widehat{Q}) = \left\{ \left[\frac{i}{k}, \frac{i+1}{k}\right] \times \left[\frac{j}{k}, \frac{j+1}{k}\right],\ 0 \le i \le k-1, 0 \le j \le k-1 \right\}. \tag{3.6}$$

Definition 3.7 (C^1 quadrilateral macro-element for $p \in \{3,4\}$)**.** Given a quadrilateral Q with vertices v_1, v_2, v_3 and v_4 and edges ε_1, ε_2, ε_3 and ε_4 we define the C^1 quadrilateral macro-element of degree $p \in \{3,4\}$ as (Q, P_Q^p, Λ_Q^p), with

(3.7)

$$P_Q^p = \left\{ \varphi : Q \to \mathbb{R},\ \text{with} \begin{array}{lll} \varphi & \in C^{p-2}(Q), & \\ (\varphi \circ \mathbf{F}_Q)|_{\hat{q}} & \in \mathbb{P}^{(p,p)}, & \text{for } 1 \le i \le 4 \\ (\varphi \circ \mathbf{F}_Q)|_{\hat{\varepsilon}_i} & \in C^{p-1}(\hat{\varepsilon}_i), & \text{and } \hat{q} \in s_{6-p}(\widehat{Q}) \\ (\partial_{\mathbf{n}_{\varepsilon_i}} \varphi \circ \mathbf{F}_Q)|_{\hat{\varepsilon}_i \cap \hat{q}} & \in \mathbb{P}^{p-1} & \end{array} \right\}$$

and

(3.8)

$$\begin{aligned} \Lambda_Q^p &= \Lambda_{0,Q} \cup \Lambda_{1,Q} \cup \Lambda_{2,Q}^p,\ \text{with} \\ \Lambda_{0,Q} &= \{\varphi(v_i), \partial_x\varphi(v_i), \partial_y\varphi(v_i), \partial_x\partial_x\varphi(v_i), \partial_x\partial_y\varphi(v_i), \partial_y\partial_y\varphi(v_i),\ 1 \le i \le 4\}, \\ \Lambda_{1,Q} &= \left\{\partial_{\mathbf{n}_{\varepsilon_i}} \varphi(m_{\varepsilon_i}),\ 1 \le i \le 4\right\}, \\ \Lambda_{2,Q}^p &= \left\{\varphi(x),\ x \in \mathcal{F}_Q^p\right\}. \end{aligned}$$

For $p = 4$ the set of face points is given as

$$\mathcal{F}_Q^4 = \left\{ \mathbf{F}_Q(\eta_1, \eta_2), \quad \eta_1, \eta_2 \in \left\{\frac{1}{4}, \frac{2}{4}, \frac{3}{4}\right\} \right\},$$

for $p = 3$ we have

$$\mathcal{F}_Q^3 = \left\{ \mathbf{F}_Q(\eta_1, \eta_2), \quad \eta_1, \eta_2 \in \left\{\frac{2}{9}, \frac{4}{9}, \frac{5}{9}, \frac{7}{9}\right\} \right\}.$$

As for $p = 5$, the degrees of freedom Λ_Q^p completely determine the functions from the space P_Q^p and the dimension is given by $\dim(P_Q^p) = |\Lambda_Q^p| = 28 + (7-p)^2$. In Fig. 4 we visualize the polynomial sub-elements from (3.7) and local degrees of freedom from (3.8) for $p \in \{3,4\}$.

3.5. **The global space and global degrees of freedom.** Using the Brenner-Sung quadrilaterals, with local spaces and degrees of freedom as defined above, we can define a global set of degrees of freedom as well as a global space. To simplify the notation we restrict ourselves here to $p \in \{3,4,5\}$.

Definition 3.8 (Global degrees of freedom)**.** Let $p \in \{3,4,5\}$. Given a quadrilateral mesh $\mathcal{M}$ we have the degrees of freedom Λ^p, given as

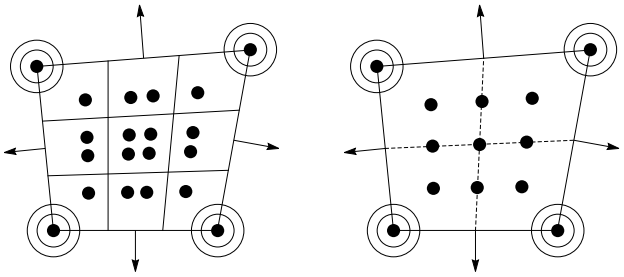

FIGURE 4. The C^1 quadrilateral macro-elements for $p = 3$ (left) and $p = 4$ (right), visualizing Λ^3_Q and Λ^4_Q, respectively. The solid inner lines represent lines of C^1 continuity, whereas the dashed lines are C^2.

- $\varphi(v)$, $\partial_x\varphi(v)$, $\partial_y\varphi(v)$, $\partial_x\partial_x\varphi(v)$, $\partial_x\partial_y\varphi(v)$ and $\partial_y\partial_y\varphi(v)$ for all vertices $v \in \mathcal{V}$;
- $\partial_{\mathbf{n}_\varepsilon}\varphi(m_\varepsilon)$ for all edge midpoints m_ε with $\varepsilon \in \mathcal{E}$; and
- $\varphi(x_Q)$ for all face points $x_Q \in \mathcal{F}^p_Q$ for all $Q \in \mathcal{Q}$.

The global degrees of freedom in Definition 3.8 together with the finite element descriptions in Definitions 3.2 and 3.7 determine a global space $\mathcal{S}^p(\mathcal{M}) \subset C^1(\Omega)$.

Lemma 3.9 (The C^1 quadrilateral space)**.** *Let $p \in \{3, 4, 5\}$ and let $\mathcal{M}$ be a quadrangulation of Ω and let the space $\mathcal{S}^p(\mathcal{M})$ be given by the degrees of freedom Λ^p as in Definition 3.8, with*

$$\mathcal{S}^p(\mathcal{M})|_Q = P^p_Q \text{ for all } Q \in \mathcal{Q},$$

where the local spaces P^p_Q are given as in Definition 3.2 or 3.7, respectively.

Then the global space satisfies $\mathcal{S}^p(\mathcal{M}) \subset C^1(\Omega)$ with

$$\varphi \in C^2(v) \text{ for all } v \in \mathcal{V},$$

for all $\varphi \in \mathcal{S}^p(\mathcal{M})$, and we have

$$\dim(\mathcal{S}^p(\mathcal{M})) = |\Lambda^p| = (7-p)^2 \cdot |\mathcal{Q}| + 1 \cdot |\mathcal{E}| + 6 \cdot |\mathcal{V}|\,.$$

Proof. Since the degrees of freedom of Λ^p corresponding to a vertex v span the C^2-data at the vertex, the smoothness $\varphi \in C^2(v)$ follows immediately. To prove $\mathcal{S}^p(\mathcal{M}) \subset C^1(\Omega)$ we consider all C^1-data along a single edge ε between two elements Q and Q'. Let $\varphi \in \mathcal{S}^p(\mathcal{M})$. We have, since $\varphi|_Q \in P^p_Q$, that $(\varphi \circ \mathbf{F}_Q)|_{\hat{\varepsilon}\cap\hat{q}} \in \mathbb{P}^p$, $(\varphi \circ \mathbf{F}_Q)|_{\hat{\varepsilon}} \in C^{p-1}$ and $(\partial_{\mathbf{n}_\varepsilon}\varphi \circ \mathbf{F}_Q)|_{\hat{\varepsilon}\cap\hat{q}} \in \mathbb{P}^{p-1}$. Consequently, since $\mathbf{F}_Q|_{\hat{\varepsilon}}$ is a linear function, we have $\varphi|_{\varepsilon\cap q} \in \mathbb{P}^p$, $\varphi|_\varepsilon \in C^{p-1}$ and $\partial_{\mathbf{n}_\varepsilon}\varphi|_{\varepsilon\cap q} \in \mathbb{P}^{p-1}$, where $\varepsilon \cap q = \varepsilon \cap \mathbf{F}_Q(\hat{q}) = \varepsilon \cap \mathbf{F}_{Q'}(\hat{q}')$. Hence, $\varphi|_\varepsilon$ is a piecewise polynomial of degree p, with dimension 6. Value, first and second derivative (in direction of the edge) of φ at the two vertices of ε are determined by the C^2-data. The function $\varphi|_\varepsilon$ is thus completely determined by the C^2-data. This is independent of the element Q, Q' under consideration. Hence, we have $\varphi \in C^0(\Omega)$. Moreover, by definition, the function $\partial_{\mathbf{n}_\varepsilon}\varphi|_\varepsilon$ is a piecewise polynomial of degree $p-1$, with dimension 5, independent of Q, Q'. Of those 5 degrees of freedom, the C^2-data at the vertices determine two each, whereas one is determined by $\partial_{\mathbf{n}_\varepsilon}\varphi(m_\varepsilon)$. Hence, $\varphi|_\varepsilon$ and $\partial_{\mathbf{n}_\varepsilon}\varphi|_\varepsilon$ are completely determined by the global degrees of freedom and $\varphi \in C^1(\Omega)$. What

remains to be shown is that $\dim(\mathcal{S}^p(\mathcal{M})) = |\Lambda^p|$. Its proof follows directly from a simple counting argument. □

We have presented Lemma 3.9 and its proof purely in terms of a finite element setting, considering the local spaces and global degrees of freedom. See [27, Section 4] for a more general statement on spline patches.

3.6. **Properties of the C^1 quadrilateral space.** Since both the degrees of freedom Λ^p_Q as well as the definition of the local space P^p_Q depend on derivatives in normal direction, the Brenner-Sung quadrilaterals and macro-element variants are not affine invariant.

The global C^1 quadrilateral space contains bivariate polynomials of total degree p.

Lemma 3.10. *We have $\mathbb{P}^p \subset \mathcal{S}^p(\mathcal{M})$.*

Proof. We need to show that for all $\psi \in \mathbb{P}^p$ as a function on Ω, it follows that $\psi \in C^1(\Omega)$, $\psi|_Q \in P^p_Q$ for all $Q \in \mathcal{Q}$ as well as $\psi \in C^2(v)$ for all $v \in \mathcal{V}$. All conditions on the continuity are trivially satisfied, since $\psi \in C^\infty$, so what remains is to show that $\psi \circ \mathbf{F}_Q \in \mathbb{P}^{(p,p)}$ and $(\partial_{\mathbf{n}_{\varepsilon_i}} \psi \circ \mathbf{F}_Q)|_{\hat{\varepsilon}_i} \in \mathbb{P}^{p-1}$ for all ε_i, according to (3.1) and (3.7). Note that we do not need to consider the sub-elements separately, as ψ is a global polynomial. The composition of a polynomial of total degree p with a bilinear function always results in a polynomial of bi-degree (p, p), hence we have $\psi \circ \mathbf{F}_Q \in \mathbb{P}^{(p,p)}$. Moreover, the directional derivative $\partial_{\mathbf{n}_{\varepsilon_i}} \psi$ is a polynomial of total degree $p-1$, restricted to an edge yields a univariate polynomial of degree $p-1$, which gives $(\partial_{\mathbf{n}_{\varepsilon_i}} \psi \circ \mathbf{F}_Q)|_{\hat{\varepsilon}_i} \in \mathbb{P}^{p-1}$. This concludes the proof. □

Since we have polynomials in the local function space and we have global degrees of freedom by functionals that take into account derivatives up to second order, we can derive an approximation error bound in Sobolev norms. To do this, we first construct a projector $\Pi_{\mathcal{S}^p(\mathcal{M})} : C^2(\overline{\Omega}) \to \mathcal{S}^p(\mathcal{M})$ as in [27], via

$$\Pi_{\mathcal{S}^p(\mathcal{M})}\varphi = \sum_{\lambda \in \Lambda^p} \lambda(\varphi)\beta_\lambda, \tag{3.9}$$

where $\beta_\lambda \in \mathcal{S}^p(\mathcal{M})$ such that it satsifies $\lambda(\beta_\lambda) = 1$ and $\lambda'(\beta_\lambda) = 0$ for all $\lambda \neq \lambda' \in \Lambda^p$. By definition of the local and global spaces and degrees of freedom, the projector has a local representation

$$\left(\Pi_{\mathcal{S}^p(\mathcal{M})}\varphi\right)|_Q = \Pi_{P^p_Q}(\varphi|_Q) = \sum_{\lambda_Q \in \Lambda^p_Q} \lambda_Q(\varphi|_Q)\beta_{\lambda_Q}, \tag{3.10}$$

where $\beta_{\lambda_Q} \in P^p_Q$ that satsifies $\lambda_Q(\beta_{\lambda_Q}) = 1$ and $\lambda'_Q(\beta_{\lambda_Q}) = 0$ for all $\lambda_Q \neq \lambda'_Q \in \Lambda^p_Q$. For a given local functional $\lambda_Q(\cdot) = \lambda(\cdot|_Q)$ we have $\beta_{\Lambda_Q} = \beta_\lambda|_Q$. Hence, the support of β_λ is given by all elements on which λ is defined, i.e., one element for all face point evaluations, two neighboring elements for all edge midpoint evaluations and, in case of vertex degrees of freedom, all elements around the vertex.

We have the following for shape regular elements.

Lemma 3.11. *Let Q be an element with $h_Q = 1$. Then the local projector satisfies*

$$\|\Pi_{P^p_Q}\psi\|_{H^2(Q)} \leq \sigma(\rho, p)\|\psi\|_{C^2(\overline{Q})}, \tag{3.11}$$

as well as

$$\|\Pi_{P_Q^p}\psi\|_{L^\infty(Q)} \leq \sigma(\rho,p)\|\psi\|_{C^2(\overline{Q})}, \tag{3.12}$$

where $\sigma(\rho,p)$ depends only on the shape regularity parameter $\rho = \rho(Q)$ and on p and where $\|\psi\|_{C^2(\overline{Q})}$ takes the supremum of all derivatives up to second order on the element Q.

The proof of this lemma is given in more detail later.

We moreover need the following standard Sobolev inequality and Bramble-Hilbert lemma.

Lemma 3.12. *Let $\psi \in H^4(Q)$. Then we have $\psi \in C^2(Q)$ and there exists a constant C_{SI}, depending on the shape regularity of Q, such that*

$$\|\psi\|_{C^2(\overline{Q})} \leq C_{SI}\|\psi\|_{H^4(Q)}$$

for all $\psi \in H^4(Q)$.

Proof. We apply [7, Lemma 4.3.4] to all derivatives of ψ up to second order, i.e., $\partial_x^{i_1}\partial_y^{i_2}\psi$ is continuous for $i_1 + i_2 \leq 2$ and

$$\|\partial_x^{i_1}\partial_y^{i_2}\psi\|_{L^\infty(Q)} \leq C\|\partial_x^{i_1}\partial_y^{i_2}\psi\|_{H^2(Q)},$$

where C is the constant from [7, Lemma 4.3.4]. Hence, all first derivatives can be bounded by $\|\psi\|_{H^3(Q)}$ and all second derivatives by $\|\psi\|_{H^4(Q)}$. Thus the desired result follows. □

Lemma 3.13 ([7, Lemma 4.3.8])**.** *Let $m \leq p+1$ and let $\varphi \in H^m(Q)$. Let $\Pi_{\mathbb{P}^p}\varphi$ be the averaged Taylor polynomial of degree p of φ over a ball B inscribed in Q. Then there exists a constant C_{BH}, depending on p and on the shape regularity of Q, such that*

$$\|\varphi - \Pi_{\mathbb{P}^p}\varphi\|_{H^m(Q)} \leq C_{BH}|\varphi|_{H^m(Q)}.$$

We can now show the following.

Theorem 3.14. *Let $Q \in \mathcal{Q}$ be an element of the mesh and let $0 \leq \ell \leq 2$ and let $4 \leq m \leq p+1$. There exists a constant $C > 0$ such that we have for all $\varphi \in H^m(Q)$*

$$\left|\varphi - \Pi_{P_Q^p}\varphi\right|_{H^\ell(Q)} \leq C\, {h_Q}^{m-\ell}\, |\varphi|_{H^m(Q)}\,,$$

where $h_Q = \max_{1\leq i\leq 4}(h_{\varepsilon_i})$. The constant C depends on the shape regularity (2.1) of Q and on p. We moreover have

$$\left\|\varphi - \Pi_{P_Q^p}\varphi\right\|_{L^\infty(Q)} \leq C\, {h_Q}^{m}\, |\varphi|_{W^m_\infty(Q)}\,.$$

Proof. The proof follows the proof of [7, Theorem 4.4.4]. Let us assume that $h_Q = 1$. We have

$$\begin{aligned}\|\varphi - \Pi_{P_Q^p}\varphi\|_{H^\ell(Q)} &\leq \|\varphi - \Pi_{\mathbb{P}^p}\varphi\|_{H^\ell(Q)} + \|\Pi_{\mathbb{P}^p}\varphi - \Pi_{P_Q^p}\varphi\|_{H^\ell(Q)} \\ &= \|\varphi - \Pi_{\mathbb{P}^p}\varphi\|_{H^\ell(Q)} + \|\Pi_{P_Q^p}(\Pi_{\mathbb{P}^p}\varphi - \varphi)\|_{H^\ell(Q)}\end{aligned}$$

Applying the bound from Lemma 3.11, of the form

$$\|\Pi_{P_Q^p}\psi\|_{H^\ell(Q)} \leq \sigma(\rho,p)\|\psi\|_{C^2(\overline{Q})}, \tag{3.13}$$

we obtain

$$\begin{aligned}\|\varphi - \Pi_{P_Q^p}\varphi\|_{H^\ell(Q)} &\leq \|\varphi - \Pi_{\mathbb{P}^p}\varphi\|_{H^\ell(Q)} + \sigma(\rho,p)\|\varphi - \Pi_{\mathbb{P}^p}\varphi\|_{C^2(\overline{Q})} \\ &\leq (1+\sigma(\rho,p)C_{SI})\|\varphi - \Pi_{\mathbb{P}^p}\varphi\|_{H^m(Q)} \\ &\leq (1+\sigma(\rho,p)C_{SI})C_{BH}|\varphi|_{H^m(Q)},\end{aligned}$$

where C_{SI} is the constant from the Sobolev inequality Lemma 3.12 and C_{BH} is the constant from the Bramble-Hilbert Lemma 3.13 (both depending on the shape regularity of Q and on p). The h-dependent estimate for general elements Q follows from a standard scaling argument. The L^∞-estimate follows the same idea as the H^ℓ-estimates, where a bound of the form

$$\|\Pi_{\mathcal{S}(\mathcal{M})}(\varphi)\|_{L^\infty(Q)} \leq \sigma(\rho,p)\|\varphi\|_{C^2(\overline{Q})}$$

is needed together with estimates similar to Lemma 3.12 and 3.13. Note that in case of the L^∞ estimate we only need $m \geq 3$, see again [7, Theorem 4.4.4]. Since Q is given such that $h_Q = 1$, the constant $\sigma(Q)$ depends only on the degree and the shape regularity constant of Q, see Lemma 3.11. This concludes the proof. □

From this local error estimate, a global estimate follows immediately.

Corollary 3.15. *Let $\mathcal{M}$ be a quadrangulation of Ω, with $\max_{\varepsilon\in\mathcal{E}}(h_\varepsilon) = h = \overline{c}\min_{\varepsilon\in\mathcal{E}}(h_\varepsilon)$. Let $0 \leq \ell \leq 2$ and let $4 \leq m \leq p+1$. There exists a constant $C > 0$, depending on the shape regularity parameter ρ, degree p and uniformity parameter $\overline{c}$, such that we have for all $\varphi \in H^m(\Omega)$*

$$\left|\varphi - \Pi_{\mathcal{S}^p(\mathcal{M})}\varphi\right|_{H^\ell(\Omega)} \leq C\, h^{m-\ell}\, |\varphi|_{H^m(\Omega)}\,,$$

as well as

$$\left\|\varphi - \Pi_{\mathcal{S}^p(\mathcal{M})}\varphi\right\|_{L^\infty(\Omega)} \leq C\, h^m\, |\varphi|_{W^m_\infty(\Omega)}\,.$$

Proof. We have, by definition,

$$\left|\varphi - \Pi_{\mathcal{S}^p(\mathcal{M})}\varphi\right|^2_{H^\ell(\Omega)} = \sum_{Q\in\mathcal{Q}} |\varphi - \Pi_{P_Q^p}(\varphi|_Q)|^2_{H^\ell(Q)}$$

for all $0 \leq \ell \leq 2$. The desired result now follows directly from Theorem 3.14. For the estimate in the L^∞-norm the sum is replaced by a maximum over all elements $Q \in \mathcal{Q}$. □

In the following Section 4 we give a constructive procedure to obtain a basis spanning the local space P_Q^p in terms of their polynomial representation on $\widehat{Q}$. We use this local representation to show the boundedness of the local projection operator.

4. Construction of a local basis

In the following we describe how to compute the basis functions corresponding to one quadrilateral Q in the mesh. We define for every vertex six basis functions to interpolate the C^2 data, for every edge we define one basis function to interpolate the normal derivative at the edge midpoint. The remaining basis functions inside the element (with vanishing traces and derivatives on the element boundary) are selected to be standard Bernstein polynomials (for $p = 5$) or standard B-splines (for $p \in \{3,4\}$). See [43, 46] for basics on B-splines.

To simplify the construction, we build a basis with respect to a slightly modified dual basis. Instead of point evaluations at the interior, we use integral-based

functionals that are dual to the Bernstein polynomials (or B-splines). Before we go into the details, we discuss the Bernstein-Bézier representation. For simplicity we first present only the case $p = 5$ and later consider the extension to lower degrees.

4.1. **Bernstein-Bézier representation of tensor-product polynomials.** Let $\hat{b}_j$ be the Bernstein polynomials of degree 5, i.e., for $0 \le j \le 5$ and $\xi \in [0,1]$,

$$\hat{b}_j(\xi) = \binom{5}{j} \xi^j (1-\xi)^{5-j}$$

and let $\hat{\mu}_i$ be the corresponding dual functionals, as in [22], i.e., $\hat{\mu}_i(\hat{b}_j) = \delta_i^j$. Let moreover

$$\mathbf{B} = \begin{pmatrix} \hat{b}_5(\xi_2) \\ \vdots \\ \hat{b}_0(\xi_2) \end{pmatrix} \begin{pmatrix} \hat{b}_0(\xi_1) & \dots & \hat{b}_5(\xi_1) \end{pmatrix}$$

be the matrix of tensor-product Bernstein basis functions spanning $\mathbb{P}^{(5,5)}$.

For each basis function $\beta \in P_Q^5$, the pull-back $\widehat{\beta} = \beta \circ \mathbf{F}_Q$ possesses a biquintic tensor-product Bernstein-Bézier representation, having the coefficients $d_{j_1,j_2} \in \mathbb{R}$,

$$\widehat{\beta}(\xi_1,\xi_2) = \beta \circ \mathbf{F}_Q(\xi_1,\xi_2) = \sum_{j_1=0}^{5} \sum_{j_2=0}^{5} d_{j_1,j_2}\, \hat{b}_{j_1,j_2}(\xi_1,\xi_2),$$

where $\hat{b}_{j_1,j_2}(\xi_1,\xi_2) = \hat{b}_{j_1}(\xi_1)\hat{b}_{j_2}(\xi_2)$. By means of a table of the form

$$\mathbf{D}[\beta] = \begin{array}{|c|c|c|c|} \hline d_{0,5} & d_{1,5} & \cdots & d_{5,5} \\ \hline \vdots & \vdots & & \vdots \\ \hline d_{0,1} & d_{1,1} & \cdots & d_{5,1} \\ \hline d_{0,0} & d_{1,0} & \cdots & d_{5,0} \\ \hline \end{array}$$

we can represent the basis function as $\widehat{\beta} = \mathbf{B} : \mathbf{D}[\beta]$, the Frobenius product of the matrix of basis functions with the coefficient matrix. Given the basis $b_{i_1,i_2} = \hat{b}_{i_1,i_2} \circ {\mathbf{F}_Q}^{-1}$ we can define a dual basis μ_{j_1,j_2} as $\mu_{j_1,j_2}(\varphi) = \hat{\mu}_{j_1} \otimes \hat{\mu}_{j_2}(\varphi \circ \mathbf{F}_Q)$, satisfying $\mu_{j_1,j_2}(b_{i_1,i_2}) = \delta_{i_1}^{j_1}\delta_{i_2}^{j_2}$.

4.2. **Relation between basis functions and dual functionals.** On each quadrilateral Q, we define 24 vertex basis functions (six for each vertex)

$$\mathrm{B}_{0,Q}^5 = \{\beta_{k,i}^0, \quad \text{for } k = 1,\dots,4 \text{ and } i = 0,\dots,5\},$$

determined by $\Lambda_{0,Q}$, four edge basis functions (one for each edge)

$$\mathrm{B}_{1,Q}^5 = \{\beta_i^1, \quad \text{for } i = 1,\dots,4\},$$

determined by $\Lambda_{1,Q}$, and four patch-interior basis functions

$$\mathrm{B}_{2,Q}^5 = \{\beta_i^2, \quad \text{for } i = 1,\dots,4\}.$$

To simplify the construction, we replace the point evaluation functionals $\Lambda_{2,Q}^5$ by the dual functionals of mapped tensor-product Bernstein polynomials

$$\mathrm{M}_{2,Q}^5 = \{\mu_{j_1,j_2}(\varphi) = \hat{\mu}_{j_1} \otimes \hat{\mu}_{j_2}(\varphi \circ \mathbf{F}_Q) : j_1, j_2 \in \{2,3\}\}.$$

We define the basis

$$\mathrm{B}_{0,Q}^5 \cup \mathrm{B}_{1,Q}^5 \cup \mathrm{B}_{2,Q}^5$$

in such a way that it is dual to

$$\Lambda_{0,Q} \cup \Lambda_{1,Q} \cup \mathrm{M}^5_{2,Q}.$$

4.3. **Patch interior basis functions.** It is clear that we have, by definition,

$$\mathrm{B}^5_{2,Q} = \{\beta^2_1, \beta^2_2, \beta^2_3, \beta^2_4\} = \{b_{2,2}, b_{2,3}, b_{3,2}, b_{3,3}\}.$$

In terms of their Bézier coefficients we have e.g.:

$$\mathbf{D}[b_{2,2}] = \begin{array}{|c|c|c|c|c|c|}\hline 0&0&0&0&0&0\\\hline 0&0&0&0&0&0\\\hline 0&0&0&0&0&0\\\hline 0&0&1&0&0&0\\\hline 0&0&0&0&0&0\\\hline 0&0&0&0&0&0\\\hline\end{array}$$

We trivially have $\mathrm{span}(\mathrm{B}^5_{2,Q}) = \ker(\Lambda_{0,Q} \cup \Lambda_{1,Q})$.

4.4. **Edge basis functions.** Let

$$\mathbf{t}^{(k)} = (t^{(k)}_1, t^{(k)}_2)^T = v_{k+1} - v_k$$

be the vector corresponding to the edge ε_k and let $a^{(k)} = \det(\mathbf{t}^{(k-1)}, \mathbf{t}^{(k)})$. Then the edge basis function β^1_1, corresponding to edge ε_1, is given by

$$\mathbf{D}[\beta^1_1] = \frac{8}{25\|\mathbf{t}^{(1)}\|} \begin{array}{|c|c|c|c|c|c|}\hline 0&0&0&0&0&0\\\hline 0&0&0&0&0&0\\\hline 0&0&0&0&0&0\\\hline 0&0&0&0&0&0\\\hline 0&0&a^{(1)}&a^{(2)}&0&0\\\hline 0&0&0&0&0&0\\\hline\end{array}$$

and analogously for β^1_2, β^1_3 and β^1_4. We have $\beta^1_j \in \ker(\Lambda^0_Q \cup \mathrm{M}^2_Q)$ and $\partial_{\mathbf{n}_{\varepsilon_i}} \beta^1_j(m_{\varepsilon_i}) = \delta^j_i$, if the normal vector $\mathbf{n}_i$ is assumed to point inwards.

4.5. **Vertex basis functions.** Before we define the coefficient matrices for the basis functions, we need to define some precomputable coefficients. We assume that all normal vectors point inwards and have

$$\mathbf{n}_{\varepsilon_k} = (n^{(k)}_1, n^{(k)}_2)^T = \frac{1}{\|\mathbf{t}^{(k)}\|}(-t^{(k)}_2, t^{(k)}_1)^T.$$

Let

$$\mathbf{q}^{(k)} = (q^{(k)}_1, q^{(k)}_2)^T = v_k - v_{k+1} + v_{k+2} - v_{k+3}$$

and moreover

$$\begin{aligned}
b^{(k)}_0 &= \tfrac{\mathbf{t}^{(k-1)}\mathbf{t}^{(k)}}{\|\mathbf{t}^{(k)}\|^2},\\
b^{(k)}_1 &= \tfrac{\mathbf{t}^{(k+1)}\mathbf{t}^{(k)}}{\|\mathbf{t}^{(k)}\|^2},\\
T^{(k)}_{i,j} &= t^{(k)}_i t^{(k)}_j,\\
Q^{(k)}_{i,j} &= t^{(k-1)}_i t^{(k)}_j + t^{(k-1)}_j t^{(k)}_i,\\
N^{(k)}_{i,j} &= n^{(k)}_i t^{(k)}_j + n^{(k)}_j t^{(k)}_i,
\end{aligned}$$

for $i, j \in \{1, 2\}$ and $k \in \{1, 2, 3, 4\}$. Here k is considered modulo 4. We define

$$\mathbf{M}_k^L = \begin{array}{|c|c|c|c|c|c|} \hline 0 & 0 & 0 & 0 & 0 & 0 \\ \hline 0 & 0 & 0 & 0 & 0 & 0 \\ \hline 0 & -\frac{3}{5}b_0^{(k-1)} & 0 & 0 & 0 & 0 \\ \hline 1 & 1+\frac{3}{5}b_1^{(k-1)} & 0 & 0 & 0 & 0 \\ \hline \frac{1}{2} & \frac{1}{2} & 0 & 0 & 0 & 0 \\ \hline 0 & 0 & 0 & 0 & 0 & 0 \\ \hline \end{array},$$

$$\mathbf{M}_k^B = \begin{array}{|c|c|c|c|c|c|} \hline 0 & 0 & 0 & 0 & 0 & 0 \\ \hline 0 & 0 & 0 & 0 & 0 & 0 \\ \hline 0 & 0 & 0 & 0 & 0 & 0 \\ \hline 0 & 0 & 0 & 0 & 0 & 0 \\ \hline 0 & \frac{1}{2} & 1+\frac{3}{5}b_0^{(k)} & -\frac{3}{5}b_1^{(k)} & 0 & 0 \\ \hline 0 & \frac{1}{2} & 1 & 0 & 0 & 0 \\ \hline \end{array}$$

and

$$\mathbf{X} = \begin{array}{|c|c|c|c|c|c|} \hline 0 & 0 & 0 & 0 & 0 & 0 \\ \hline 0 & 0 & 0 & 0 & 0 & 0 \\ \hline 0 & 0 & 0 & 0 & 0 & 0 \\ \hline 0 & 0 & 0 & 0 & 0 & 0 \\ \hline \frac{1}{2} & 0 & 0 & 0 & 0 & 0 \\ \hline 1 & \frac{1}{2} & 0 & 0 & 0 & 0 \\ \hline \end{array}.$$

The vertex basis function $\beta_{1,0}^0$ is then given by

$$\mathbf{D}[\beta_{1,0}^0] = \mathbf{M}_1^L + \mathbf{M}_1^B + \mathbf{X}.$$

In general, the basis functions $\beta_{k,0}^0$ are given by

$$\mathbf{D}[\beta_{k,0}^0] = R_k(\mathbf{M}_k^L + \mathbf{M}_k^B + \mathbf{X})$$

where R_k is a suitable operator $R_k : \mathbb{R}^{6\times 6} \to \mathbb{R}^{6\times 6}$ taking care of the local reparametrization, rotating the positions of the vertices. Let

$$\mathbf{Y}_{k,i} = \begin{array}{|c|c|c|c|c|c|} \hline 0 & 0 & 0 & 0 & 0 & 0 \\ \hline 0 & 0 & 0 & 0 & 0 & 0 \\ \hline 0 & 0 & 0 & 0 & 0 & 0 \\ \hline 0 & -\frac{1}{5}t_i^{(k-2)} & 0 & 0 & 0 & 0 \\ \hline 0 & \frac{1}{10}q_i^{(k)} & \frac{1}{5}t_i^{(k+1)} & 0 & 0 & 0 \\ \hline 0 & 0 & 0 & 0 & 0 & 0 \\ \hline \end{array}$$

then the vertex basis functions $\beta_{k,1}^0$ and $\beta_{k,2}^0$ interpolating the derivatives in x- and y-direction, respectively, are given by

$$\begin{aligned} \mathbf{D}[\beta_{k,i}^0] = \quad & \tfrac{2}{5}R_k\left(-t_i^{(k-1)}\mathbf{M}_k^L + t_i^{(k)}\mathbf{M}_k^B + \mathbf{Y}_{k,i}\right) \\ & -\tfrac{5}{16}n_i^{(k)}\mathbf{D}[\beta_k^1] - \tfrac{5}{16}n_i^{(k-1)}\mathbf{D}[\beta_{k-1}^1], \end{aligned}$$

for $i = 1, 2$. Finally we define the vertex basis functions $\beta^0_{k,3}$, $\beta^0_{k,4}$ and $\beta^0_{k,5}$, interpolating the second derivatives. Let

$$\mathbf{Z}_{k,(i,j)} = \begin{array}{|c|c|c|c|c|c|}\hline 0 & 0 & 0 & 0 & 0 & 0 \\ \hline 0 & 0 & 0 & 0 & 0 & 0 \\ \hline 0 & 0 & 0 & 0 & 0 & 0 \\ \hline 0 & \frac{1}{5}Q^{(k-1)}_{i,j} & 0 & 0 & 0 & 0 \\ \hline -\frac{1}{2}T^{(k-1)}_{i,j} & -\frac{2}{5}Q^{(k)}_{i,j} - \frac{1}{2}T^{(k-1)}_{i,j} - \frac{1}{2}T^{(k)}_{i,j} & \frac{1}{5}Q^{(k+1)}_{i,j} & 0 & 0 & 0 \\ \hline 0 & -\frac{1}{2}T^{(k)}_{i,j} & 0 & 0 & 0 & 0 \\ \hline \end{array},$$

then we have

$$\begin{aligned}\mathbf{D}[\beta^0_{k,i+j+1}] = \quad & \tfrac{\lambda}{20} R_k \left(T^{(k-1)}_{i,j} \mathbf{M}^L_k + T^{(k)}_{i,j} \mathbf{M}^B_k + \mathbf{Z}_{k,(i,j)} \right) \\ & - \tfrac{\lambda}{32} N^{(k)}_{i,j} \mathbf{D}[\beta^1_k] + \tfrac{\lambda}{32} N^{(k-1)}_{i,j} \mathbf{D}[\beta^1_{k-1}]\end{aligned}$$

for $i, j \in \{1, 2\}$, where $\lambda = 2 - \delta^j_i$. All representations of basis functions can be verified using simple symbolic computations. We have $\beta^0_{k,j} \in \ker(\Lambda_{1,Q} \cup \mathrm{M}^5_{2,Q})$ and

$$(\beta^0_{k,0}, \beta^0_{k,1}, \beta^0_{k,2}, \beta^0_{k,3}, \beta^0_{k,4}, \beta^0_{k,5})$$

being dual to

$$(\varphi(v_k), \partial_x\varphi(v_k), \partial_y\varphi(v_k), \partial_x\partial_x\varphi(v_k), \partial_x\partial_y\varphi(v_k), \partial_y\partial_y\varphi(v_k)),$$

with vanishing C^2-data at all other vertices.

5. The C^1 quadrilateral macro-element

We can extend the definition of polynomial Brenner-Sung quadrilaterals of degree $p \geq 5$ to certain B-spline based macro-elements of any degree $p \geq 3$. In that case the degrees of freedom are given as C^2-data in the vertices, normal derivative and point data at certain points along the edges, as well as suitably many interior functions that have vanishing values and gradients at all element boundaries. In such a setting, refinement can be performed either by splitting the macro-elements or by knot insertion within every macro-element. Note that, in the construction below, the continuity within the macro-element is of order $p - 2$ for all degrees. In general, any order $1 \leq r \leq p - 2$ can be achieved.

5.1. The general setting of C^1 quadrilateral spline macro-elements.

We assume that every quadrilateral Q is split into $k \times k$ elements by mapping a regular split of the parameter domain $\widehat{Q} = [0, 1]^2$ using $\mathbf{F}_Q$. Let $\mathcal{S}^{p,r}_k$ be the univariate B-spline space of degree p and regularity r over the interval $[0, 1]$ split into k polynomial segments of the same length, i.e., having the knot vector

$$\left(0, \ldots, 0, \frac{1}{k}, \frac{1}{k}, \frac{2}{k}, \frac{2}{k}, \ldots, \frac{k-1}{k}, \frac{k-1}{k}, 1, \ldots, 1\right)$$

for $r = p - 2$ and

$$\left(0, \ldots, 0, \frac{1}{k}, \frac{2}{k}, \ldots, \frac{k-1}{k}, 1, \ldots, 1\right)$$

for $r = p - 1$, where the first and last knots are repeated $p + 1$ times. These knot vectors define piecewise polynomials on the split $s_k(\widehat{Q})$ in the tensor-product case. Let θ^p_i, for $i = 0, \ldots, 2k+p-2$ and η^p_i, for $i = 0, \ldots, k+p-1$, be the corresponding Greville abscissae for the first and second knot vector, respectively. Note that the

Greville abscissae γ_i corresponding to a given knot vector $(\xi_0, \dots, \xi_N)$ are defined as knot averages $\gamma_i = (\xi_{i+1} + \cdots + \xi_{i+p})/p$ for $i = 0, \dots, N-p-1$.

As in Definition 3.2 we can define the local function space and the local degrees of freedom, where we need to assume $k \geq \max(1, 6-p)$ in order to be able to split the vertex degrees of freedom.

Definition 5.1 (Local space and degrees of freedom)**.** Given a quadrilateral Q with vertices v_1, v_2, v_3 and v_4 we define the C^1 quadrilateral spline macro-element of degree p as (Q, P_Q, Λ_Q), with

$$P_Q = \left\{ \varphi : Q \to \mathbb{R}, \text{ with } \begin{array}{ll} (\varphi \circ \mathbf{F}_Q) & \in \mathcal{S}_k^{p,p-2} \otimes \mathcal{S}_k^{p,p-2}, \\ (\varphi \circ \mathbf{F}_Q)|_{\hat{\varepsilon}} & \in \mathcal{S}_k^{p,p-1}, \\ (\partial_{\mathbf{n}_\varepsilon} \varphi \circ \mathbf{F}_Q)|_{\hat{\varepsilon}} & \in \mathcal{S}_k^{p-1,p-2}, \end{array} \text{ for each } \varepsilon \text{ of } Q \right\}$$

and

$$\begin{aligned} \Lambda_Q &= \Lambda_{0,Q} \cup \Lambda_{1,Q}^* \cup \Lambda_{2,Q}^*, \text{ with} \\ \Lambda_{0,Q} &= \{\varphi(v_i), \partial_x\varphi(v_i), \partial_y\varphi(v_i), \partial_x\partial_x\varphi(v_i), \partial_x\partial_y\varphi(v_i), \partial_y\partial_y\varphi(v_i),\ 1 \leq i \leq 4\}, \\ \Lambda_{1,Q}^* &= \{\varphi(r_{i,j_0}),\ \text{ for } 1 \leq i \leq 4,\ 1 \leq j_0 \leq k+p-6\} \\ &\qquad \cup \left\{\partial_{\mathbf{n}_{\varepsilon_i}} \varphi(q_{i,j_1}),\ \text{ for } 1 \leq i \leq 4,\ 1 \leq j_1 \leq k+p-5\right\}, \\ \Lambda_{2,Q}^* &= \left\{\varphi(x),\ x \in \mathcal{F}_Q^*\right\}. \end{aligned}$$

Here $r_{i,j_0} = \mathbf{F}_{\varepsilon_i}(\eta_{j_0+2}^p)$, $q_{i,j_1} = \mathbf{F}_{\varepsilon_i}(\eta_{j_1+1}^{p-1})$, with $\mathbf{F}_{\varepsilon_i} = \mathbf{F}_Q|_{\varepsilon_i}$, and the set of face points is given as

$$\mathcal{F}_Q^* = \left\{\mathbf{F}_Q\left(\theta_i^p, \theta_j^p\right), 2 \leq i, j \leq 2k+p-4\right\}.$$

5.2. **The special cases for $p = 3$ and $p = 4$ as in Definition 3.7.** In this section we present in more detail the two special cases of C^1 quadrilateral macro-elements presented in Definition 3.7. Since we need $k \geq \max(1, 6-p)$, they represent the spline elements with the least number of inner knots, allowing a separation of degrees of freedom at the vertices. For $p = 4$ we consider the spline space with one inner knot at $\frac{1}{2}$ with multiplicity two in each direction $\mathcal{S}_2^{4,2} \otimes \mathcal{S}_2^{4,2}$, having the basis $\hat{b}_{j_1,j_2}^4$ and corresponding dual basis $\hat{\mu}_{j_1,j_2}^4$ for $0 \leq j_1, j_2 \leq 6$. For $p = 3$ we consider the spline space $\mathcal{S}_3^{3,1} \otimes \mathcal{S}_3^{3,1}$, with basis $\hat{b}_{j_1,j_2}^3$ and dual basis $\hat{\mu}_{j_1,j_2}^3$ for $0 \leq j_1, j_2 \leq 7$, see [43, 46].

Hence, for smaller degrees that patches Q are macro-elements with 2×2 (for $p = 4$) or 3×3 (for $p = 3$) polynomial sub-elements. Let $n = 11 - p$. We write, as for $p = 5$, all tensor-product basis functions in a matrix

$$\mathbf{B} = \begin{pmatrix} \hat{b}_{0,n-1}^p & \dots & \hat{b}_{n-1,n-1}^p \\ \vdots & & \vdots \\ \hat{b}_{0,0}^p & \dots & \hat{b}_{n-1,0}^p \end{pmatrix}$$

and denote again with $\mathbf{D}[\beta]$ the $(n \times n)$-matrix of coefficients. As for $p = 5$, let $b_{j_1,j_2}^p = \hat{b}_{j_1,j_2}^p \circ {\mathbf{F}_Q}^{-1}$ denote the basis functions on the element Q.

5.3. **Patch interior basis functions for $p = 3$ and $p = 4$.** We have $(n-4)^2$ basis functions

$$\mathrm{B}_{2,Q}^p = \{b_{j_1,j_2}^p,\ 2 \leq j_1, j_2 \leq n-3\},$$

which satisfy $\operatorname{span}(\mathrm{B}_{2,Q}^p) = \ker(\Lambda_{0,Q} \cup \Lambda_{1,Q})$.

5.4. **Edge basis functions for $p = 3$ and $p = 4$.** The edge basis function β_1^1, corresponding to edge ε_1, is given for $p = 4$ by

$$\mathbf{D}[\beta_1^1] = \frac{1}{32\|\mathbf{t}^{(1)}\|} \begin{array}{|c|c|c|c|c|c|c|} \hline 0 & 0 & 0 & 0 & 0 & 0 & 0 \\ \hline 0 & 0 & 0 & 0 & 0 & 0 & 0 \\ \hline 0 & 0 & 0 & 0 & 0 & 0 & 0 \\ \hline 0 & 0 & 0 & 0 & 0 & 0 & 0 \\ \hline 0 & 0 & 0 & 0 & 0 & 0 & 0 \\ \hline 0 & 0 & 2a^{(1)} & 3a^{(1)} + 3a^{(2)} & 2a^{(2)} & 0 & 0 \\ \hline 0 & 0 & 0 & 0 & 0 & 0 & 0 \\ \hline \end{array},$$

and for $p = 3$ by

$$\mathbf{D}[\beta_1^1] = \frac{2}{81\|\mathbf{t}^{(1)}\|} \begin{array}{|c|c|c|c|c|c|c|} \hline 0 & 0 & 0 & 0 & 0 & 0 & 0 \\ \hline 0 & 0 & 0 & 0 & 0 & 0 & 0 \\ \hline 0 & 0 & 0 & 0 & 0 & 0 & 0 \\ \hline 0 & 0 & 0 & 0 & 0 & 0 & 0 \\ \hline 0 & 0 & 0 & 0 & 0 & 0 & 0 \\ \hline 0 & 0 & 0 & 0 & 0 & 0 & 0 \\ \hline 0 & 0 & a^{(1)} & 3a^{(1)} + 2a^{(2)} & 2a^{(1)} + 3a^{(2)} & a^{(2)} & 0 \\ \hline 0 & 0 & 0 & 0 & 0 & 0 & 0 \\ \hline \end{array}.$$

The functions β_2^1, β_3^1 and β_4^1 are defined analogously. Analogously to the polynomial case, we have $\beta_j^1 \in \ker(\Lambda_{0,Q} \cup \mathrm{M}_{2,Q}^p)$ and $\partial_{\mathbf{n}_{\varepsilon_i}} \beta_j^1(m_{\varepsilon_i}) = \delta_i^j$, if the normal vector $\mathbf{n}_i$ is assumed to point inwards.

5.5. **Vertex basis functions for $p = 4$.** We define

$$\mathbf{M}_k^L = \begin{array}{|c|c|c|c|c|c|c|} \hline 0 & 0 & 0 & 0 & 0 & 0 & 0 \\ \hline 0 & 0 & 0 & 0 & 0 & 0 & 0 \\ \hline 0 & -\frac{1}{8} b_0^{(k-1)} & 0 & 0 & 0 & 0 & 0 \\ \hline \frac{1}{2} & \frac{1}{2} + \frac{3}{16}(b_1^{(k-1)} - b_0^{(k-1)}) & 0 & 0 & 0 & 0 & 0 \\ \hline \frac{2}{3} & \frac{2}{3} + \frac{1}{8} b_1^{(k-1)} & 0 & 0 & 0 & 0 & 0 \\ \hline \frac{1}{3} & \frac{1}{3} & 0 & 0 & 0 & 0 & 0 \\ \hline 0 & 0 & 0 & 0 & 0 & 0 & 0 \\ \hline \end{array},$$

$$\mathbf{M}_k^B = \begin{array}{|c|c|c|c|c|c|c|} \hline 0 & 0 & 0 & 0 & 0 & 0 & 0 \\ \hline 0 & 0 & 0 & 0 & 0 & 0 & 0 \\ \hline 0 & 0 & 0 & 0 & 0 & 0 & 0 \\ \hline 0 & 0 & 0 & 0 & 0 & 0 & 0 \\ \hline 0 & 0 & 0 & 0 & 0 & 0 & 0 \\ \hline 0 & \frac{1}{3} & \frac{2}{3} + \frac{1}{8} b_0^{(k)} & \frac{1}{2} + \frac{3}{16}(b_0^{(k)} - b_1^{(k)}) & -\frac{1}{8} b_1^{(k)} & 0 & 0 \\ \hline 0 & \frac{1}{3} & \frac{2}{3} & \frac{1}{2} & 0 & 0 & 0 \\ \hline \end{array}$$

and

$$\mathbf{X} = \begin{array}{|c|c|c|c|c|c|c|}\hline 0&0&0&0&0&0&0\\\hline 0&0&0&0&0&0&0\\\hline 0&0&0&0&0&0&0\\\hline 0&0&0&0&0&0&0\\\hline \frac{1}{3}&\frac{1}{3}&0&0&0&0&0\\\hline \frac{2}{3}&\frac{1}{3}&\frac{1}{3}&0&0&0&0\\\hline 1&\frac{2}{3}&\frac{1}{3}&0&0&0&0\\\hline\end{array}.$$

The basis functions $\beta^0_{k,0}$ are given by

$$\mathbf{D}[\beta^0_{k,0}] = R_k(\mathbf{M}^L_k + \mathbf{M}^B_k + \mathbf{X}).$$

Let

$$\mathbf{Y}_{k,i} = \begin{array}{|c|c|c|c|c|c|c|}\hline 0&0&0&0&0&0&0\\\hline 0&0&0&0&0&0&0\\\hline 0&0&0&0&0&0&0\\\hline 0&-\frac{1}{24}t_i^{(k-2)}&0&0&0&0&0\\\hline 0&-\frac{1}{4}t_i^{(k-2)}-\frac{1}{6}q_i^{(k)}&0&0&0&0&0\\\hline 0&\frac{1}{24}q_i^{(k)}&\frac{1}{4}t_i^{(k+1)}-\frac{1}{6}q_i^{(k)}&\frac{1}{24}t_i^{(k+1)}&0&0&0\\\hline 0&0&0&0&0&0&0\\\hline\end{array},$$

then the vertex basis functions $\beta^0_{k,1}$ and $\beta^0_{k,2}$ are given by

$$\begin{aligned}\mathbf{D}[\beta^0_{k,i}] = \quad & \tfrac{3}{8}R_k\left(-t_i^{(k-1)}\mathbf{M}^L_k + t_i^{(k)}\mathbf{M}^B_k + \mathbf{Y}_{k,i}\right)\\ & -\tfrac{1}{4}n_i^{(k)}\mathbf{D}[\beta^1_k] - \tfrac{1}{4}n_i^{(k-1)}\mathbf{D}[\beta^1_{k-1}],\end{aligned}$$

for $i = 1, 2$. Let

$\mathbf{Z}_{k,(i,j)} =$

$$\begin{array}{|c|c|c|c|c|c|}\hline 0&0&0&0&0&\dots\\\hline 0&0&0&0&0&\\\hline 0&0&0&0&0&\\\hline 0&\frac{1}{32}Q_{i,j}^{(k-1)}&0&0&0&\\\hline -\frac{1}{6}T_{i,j}^{(k-1)}&-\frac{1}{6}T_{i,j}^{(k-1)}-\frac{1}{8}Q_{i,j}^{(k)}+\frac{1}{16}Q_{i,j}^{(k-1)}&0&0&0&\\\hline -\frac{1}{3}T_{i,j}^{(k-1)}&-\frac{1}{3}T_{i,j}^{(k-1)}-\frac{1}{3}T_{i,j}^{(k)}-\frac{3}{16}Q_{i,j}^{(k)}&-\frac{1}{6}T_{i,j}^{(k)}-\frac{1}{8}Q_{i,j}^{(k)}+\frac{1}{16}Q_{i,j}^{(k+1)}&\frac{1}{32}Q_{i,j}^{(k+1)}&0&\\\hline 0&-\frac{1}{3}T_{i,j}^{(k)}&-\frac{1}{6}T_{i,j}^{(k)}&0&0&\dots\\\hline\end{array},$$

then we have

$$\begin{aligned}\mathbf{D}[\beta^0_{k,i+j+1}] = \quad & \tfrac{\lambda}{24}R_k\left(T_{i,j}^{(k-1)}\mathbf{M}^L_k + T_{i,j}^{(k)}\mathbf{M}^B_k + \mathbf{Z}_{k,(i,j)}\right)\\ & -\tfrac{\lambda}{48}N_{i,j}^{(k)}\mathbf{D}[\beta^1_k] + \tfrac{\lambda}{48}N_{i,j}^{(k-1)}\mathbf{D}[\beta^1_{k-1}]\end{aligned}$$

for $i, j \in \{1, 2\}$, where $\lambda = 2 - \delta^j_i$. We have $\beta^0_{k,j} \in \ker(\Lambda_{1,Q} \cup \mathrm{M}^4_{2,Q})$ and $\{\beta^0_{k,j}\}_{k=1,\dots,4,j=0,\dots,5}$ being dual to $\Lambda_{0,Q}$.

5.6. **Vertex basis functions for $p = 3$.** We define

$\mathbf{M}_k^L =$

0	0	0	0	0	0	0	0
0	0	0	0	0	0	0	0
0	$-\frac{1}{18}b_0^{(k-1)}$	0	0	0	0	0	0
$\frac{1}{3}$	$\frac{1}{3}+\frac{1}{9}b_1^{(k-1)}-\frac{1}{6}b_0^{(k-1)}$	0	0	0	0	0	0
$\frac{2}{3}$	$\frac{2}{3}+\frac{1}{6}b_1^{(k-1)}-\frac{1}{9}b_0^{(k-1)}$	0	0	0	0	0	0
$\frac{2}{3}$	$\frac{2}{3}+\frac{1}{18}b_1^{(k-1)}$	0	0	0	0	0	0
$\frac{1}{3}$	$\frac{1}{3}$	0	0	0	0	0	0
0	0	0	0	0	0	0	0

,

$\mathbf{M}_k^B =$

0	0	0	0	0	0	0	0
0	0	0	0	0	0	0	0
0	0	0	0	0	0	0	0
0	0	0	0	0	0	0	0
0	0	0	0	0	0	0	0
0	0	0	0	0	0	0	0
0	$\frac{1}{3}$	$\frac{2}{3}+\frac{1}{18}b_0^{(k)}$	$\frac{2}{3}+\frac{1}{6}b_0^{(k)}-\frac{1}{9}b_1^{(k)}$	$\frac{1}{3}+\frac{1}{9}b_0^{(k)}-\frac{1}{6}b_1^{(k)}$	$-\frac{1}{18}b_1^{(k)}$	0	0
0	$\frac{1}{3}$	$\frac{2}{3}$	$\frac{2}{3}$	$\frac{1}{3}$	0	0	0

and

$$\mathbf{X} = \begin{array}{|c|c|c|c|c|c|c|c|}\hline 0&0&0&0&0&0&0&0\\\hline 0&0&0&0&0&0&0&0\\\hline 0&0&0&0&0&0&0&0\\\hline 0&0&0&0&0&0&0&0\\\hline 0&0&0&0&0&0&0&0\\\hline \frac{1}{3}&\frac{1}{3}&0&0&0&0&0&0\\\hline \frac{2}{3}&\frac{1}{3}&\frac{1}{3}&0&0&0&0&0\\\hline 1&\frac{2}{3}&\frac{1}{3}&0&0&0&0&0\\\hline\end{array}.$$

The basis functions $\beta_{k,0}^0$ are given by

$$\mathbf{D}[\beta_{k,0}^0] = R_k(\mathbf{M}_k^L + \mathbf{M}_k^B + \mathbf{X}).$$

Let

$\mathbf{Y}_{k,i} =$

0	0	0	0	0	0	0	0
0	0	0	0	0	0	0	0
0	0	0	0	0	0	0	0
0	0	0	0	0	0	0	0
0	$-\frac{1}{18}t_i^{(k-2)}-\frac{1}{54}q_i^{(k)}$	0	0	0	0	0	0
0	$-\frac{5}{18}t_i^{(k-2)}-\frac{11}{54}q_i^{(k)}$	0	0	0	0	0	0
0	$\frac{1}{27}q_i^{(k)}$	$\frac{5}{18}t_i^{(k+1)}-\frac{11}{54}q_i^{(k)}$	$\frac{1}{18}t_i^{(k+1)}-\frac{1}{54}q_i^{(k)}$	0	0	0	0
0	0	0	0	0	0	0	0

then the vertex basis functions $\beta^0_{k,1}$ and $\beta^0_{k,2}$ are given by

$$\begin{aligned}\mathbf{D}[\beta^0_{k,i}] = \quad & \tfrac{1}{3}R_k\left(-t_i^{(k-1)}\mathbf{M}_k^L + t_i^{(k)}\mathbf{M}_k^B + \mathbf{Y}_{k,i}\right)\\ & -\tfrac{1}{8}n_i^{(k)}\mathbf{D}[\beta^1_k] - \tfrac{1}{8}n_i^{(k-1)}\mathbf{D}[\beta^1_{k-1}],\end{aligned}$$

for $i = 1, 2$. Let

$\mathbf{Z}_{k,(i,j)} =$

0	0	0	0	0	...
0	0	0	0	0	
0	0	0	0	0	
0	0	0	0	0	
0	$-\frac{1}{72}Q^{(k)}_{i,j} + \frac{1}{36}Q^{(k-1)}_{i,j}$	0	0	0	
$-\frac{1}{6}T^{(k-1)}_{i,j}$	$-\frac{1}{6}T^{(k-1)}_{i,j} - \frac{11}{72}Q^{(k)}_{i,j} + \frac{1}{18}Q^{(k-1)}_{i,j}$	0	0	0	
$-\frac{1}{3}T^{(k-1)}_{i,j}$	$-\frac{1}{3}T^{(k)}_{i,j} - \frac{1}{3}T^{(k-1)}_{i,j} - \frac{1}{6}Q^{(k)}_{i,j}$	$-\frac{1}{6}T^{(k)}_{i,j} - \frac{11}{72}Q^{(k)}_{i,j} + \frac{1}{18}Q^{(k+1)}_{i,j}$	$-\frac{1}{72}Q^{(k)}_{i,j} + \frac{1}{36}Q^{(k+1)}_{i,j}$	0	
0	$-\frac{1}{3}T^{(k)}_{i,j}$	$-\frac{1}{6}T^{(k)}_{i,j}$	0	0	...

,

then we have

$$\begin{aligned}\mathbf{D}[\beta^0_{k,i+j+1}] = \quad & \tfrac{\lambda}{27}R_k\left(T_{i,j}^{(k-1)}\mathbf{M}_k^L + T_{i,j}^{(k)}\mathbf{M}_k^B + \mathbf{Z}_{k,(i,j)}\right)\\ & -\tfrac{\lambda}{96}N_{i,j}^{(k)}\mathbf{D}[\beta^1_k] + \tfrac{\lambda}{96}N_{i,j}^{(k-1)}\mathbf{D}[\beta^1_{k-1}]\end{aligned}$$

for $i, j \in \{1, 2\}$, where $\lambda = 2 - \delta_i^j$. We have $\beta^0_{k,j} \in \ker(\Lambda_{1,Q} \cup \mathrm{M}^3_{2,Q})$ and $\{\beta^0_{k,j}\}_{k=1,\dots,4,j=0,\dots,5}$ being dual to $\Lambda_{0,Q}$.

5.7. **Boundedness of the local projector.** As for $p = 5$, all representations of basis functions for $p \in \{3, 4\}$ can be verified using simple symbolic computations. We now have all the ingredients to show the boundedness of the finite element projector.

Proof of Lemma 3.11. Here we consider only $p \in \{3, 4, 5\}$, the proof follows the same steps for higher degrees. Let $h_Q = 1$. Then we trivially have $t_i^k \le 1$ and $\frac{1}{\|\mathbf{t}^{(k)}\|^2} \le \frac{1}{\rho}$. Hence, all coefficients of all basis functions $\beta \in \mathrm{B}^p_{0,Q} \cup \mathrm{B}^p_{1,Q} \cup \mathrm{B}^p_{2,Q}$ are bounded depending on ρ and the Bernstein polynomials form a partition of unity we have

$$\|\beta\|_{L^\infty(Q)} \le \sigma'(\rho, p), \text{ for all } \beta \in \mathrm{B}^p_{0,Q} \cup \mathrm{B}^p_{1,Q} \cup \mathrm{B}^p_{2,Q}, \tag{5.1}$$

for some constant $\sigma'(\rho, p)$ depending only on ρ and p. The same is true for the L^2-norm and also for the H^1- and H^2-seminorms, since all derivatives can be interpreted as differences of coefficients in a Bernstein/B-spline basis of lower degree and the integration domain is bounded as well. Recall that the basis $\mathrm{B}^p_{0,Q} \cup \mathrm{B}^p_{1,Q} \cup \mathrm{B}^p_{2,Q}$ is dual to $\Lambda_{0,Q} \cup \Lambda_{1,Q} \cup \mathrm{M}^p_{2,Q}$. The basis transformation to obtain a basis dual to $\Lambda^p_{2,Q}$ also depends only on ρ and p. Hence, the desired result follows immediately. □

6. Extension to isoparametric/isogeometric elements

As pointed out before, the Brenner-Sung quadrilaterals and related spline macro-elements are not affine invariant. Hence their definition depends on the underlying geometry. It is possible to extend the construction from bilinearly mapped quadrilaterals Q, with $\mathbf{F}_Q \in (\mathbb{P}^{(1,1)})^2$, to fully isoparametric elements, with $\mathbf{F}_Q \in (P^p_Q)^2$. However, this has to be done with some additional care. A fitting approach for

curved boundaries is employed for spline patches (macro-elements) with Argyris-like degrees of freedom in [25]. In this paper we focus on the purely quadrilateral case. Modifications of elements near curved boundaries were also discussed and resolved successfully in [4]. However, there the authors presented the construction of a minimal determining set (similar to a dual basis), without giving an explicit basis representation. Moreover, a complete analysis of the convergence in case of local modifications near the boundary is not known and beyond the scope of the current paper. It is important to note, that a suitable splitting of elements can increase the flexibility of the resulting space, such as in [20], where using a regular 4-split on degree $p = 5$ triangular elements allows for the construction of surfaces of arbitrary topology.

7. Numerical examples

The goal is to demonstrate the potential of using the proposed C^1 spaces over quadrilateral meshes $\mathcal{M}$ for solving fourth order PDEs over domains Ω with piecewise linear boundary. This is done on the basis of a particular example, namely for the biharmonic equation

$$\begin{cases} \triangle^2 u(\mathbf{x}) &= g(\mathbf{x}) \quad \mathbf{x} \in \Omega \\ u(\mathbf{x}) &= g_1(\mathbf{x}) \quad \mathbf{x} \in \partial\Omega \\ \frac{\partial u}{\partial \mathbf{n}}(\mathbf{x}) &= g_2(\mathbf{x}) \quad \mathbf{x} \in \partial\Omega. \end{cases} \tag{7.1}$$

More precisely, we solve problem (7.1) via a standard Galerkin discretization by employing the family of C^1 quadrilateral spaces $\mathcal{S}^p(\mathcal{M}_h)$, where the mesh size h denotes the length of the longest edge in $\mathcal{M}_h$, with $h = h_0 \frac{1}{2^L}$, $L = 0, 1, \ldots, 5$. Here L denotes the level of refinement, h_0 is the mesh size of the initial mesh $\mathcal{M}$, and $\mathcal{M}_h = (\mathcal{Q}_h, \mathcal{E}_h, \mathcal{V}_h)$ is the resulting refined quadrilateral mesh obtained from $\mathcal{M}$ with corresponding sets of quadrilaterals $\mathcal{Q}_h$, edges $\mathcal{E}_h$ and vertices $\mathcal{V}_h$. Note that in the refinement process, each quadrilateral of the current mesh is split regularly into four sub-quadrilaterals. Moreover, in all examples below, the functions g, g_1 and g_2 from problem (7.1) are computed from an exact solution u, and the resulting Dirichlet boundary data g_1 and g_2 are L^2 projected and strongly imposed to the numerical solution $u_h \in \mathcal{S}^p(\mathcal{M}_h)$.

Example 7.1. For the two meshes $\mathcal{M}$ in Fig. 5 and Fig. 6, which are visualized in the top left of each figure, we solve the biharmonic equation (7.1) over the corresponding bilinear multi-patch domains by using the Brenner-Sung quadrilateral and macro-element spaces $\mathcal{S}^p(\mathcal{M}_h)$ for polynomial degrees $p = 3, 4, 5$. For both cases, the considered exact solution is given by

$$u(x_1, x_2) = -4 \cos(\frac{x_1}{2}) \sin(\frac{x_2}{2}), \tag{7.2}$$

and is shown in Fig. 5 (top row, right) and Fig. 6 (top row, right), respectively. The resulting L^∞-error as well as the relative L^2, H^1 and H^2-errors with respect to the number of degrees of freedom (NDOF) are shown in the middle and bottom rows of Fig. 5 and Fig. 6, and decrease for both examples with optimal order of $\mathcal{O}(h^{p+1})$, $\mathcal{O}(h^{p+1})$, $\mathcal{O}(h^p)$ and $\mathcal{O}(h^{p-1})$, respectively.

Example 7.2. We compare the C^1 quadrilateral spaces $\mathcal{S}^p(\mathcal{M}_h)$ for polynomial degrees $p = 3, 4, 5$ as constructed in this paper with the C^1 isogeometric spaces $\mathcal{A}_h$ for the cases $(p, r) = (3, 1)$, $(p, r) = (4, 2)$ and $(p, r) = (5, 3)$ as generated in [27]

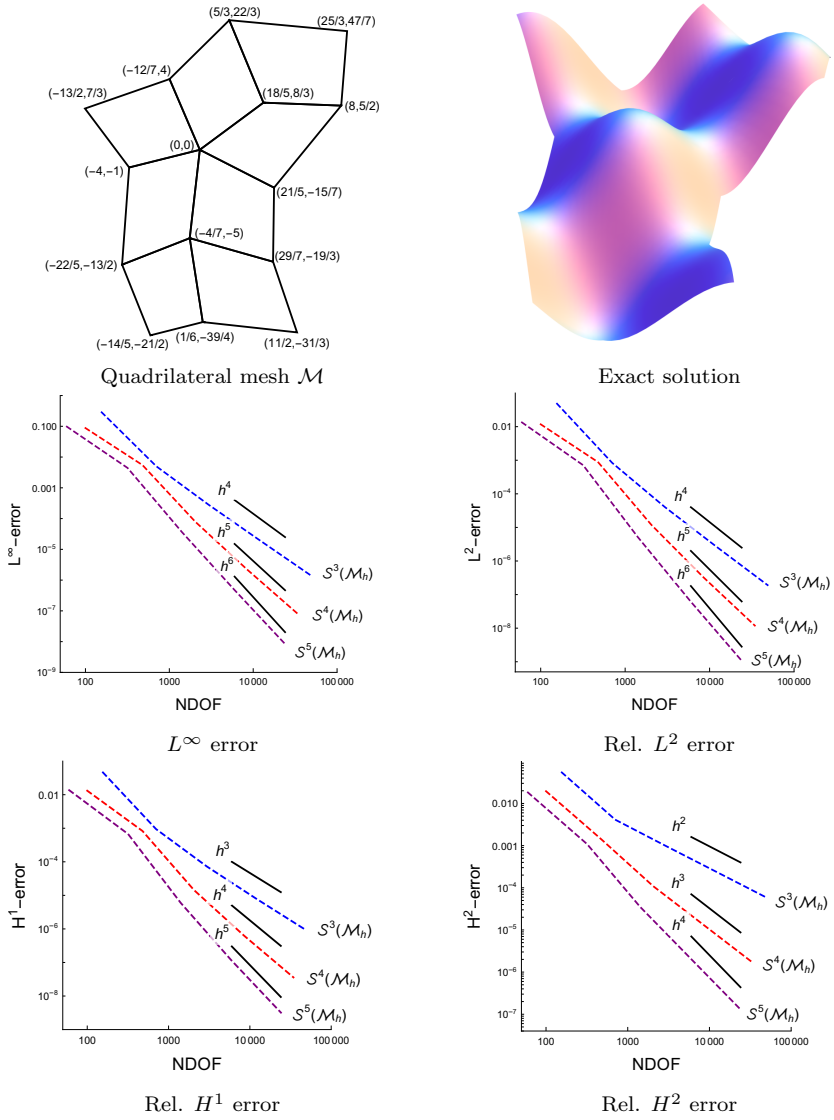

FIGURE 5. Solving the biharmonic equation (7.1) on the given quadrilateral mesh $\mathcal{M}$ (top row, left) for the exact solution (7.2) (top row, right) with the resulting L^∞ and relative L^2, H^1, H^2-errors (middle and bottom row). See Example 7.1.

by means of standard h-refinement. For this purpose, we solve the biharmonic equation (7.1) for the exact solution

$$u(x_1, x_2) = -4\cos(\frac{x_1}{2})\sin(\frac{x_2}{2}), \tag{7.3}$$

see Fig. 7 (top row, right), on the bilinarly parameterized multi-patch domain Ω determined by the mesh $\mathcal{M}$ shown in Fig. 7 (top row, left). The resulting L^∞-error as well as the relative L^2, H^1 and H^2-errors, which are reported in Fig. 7

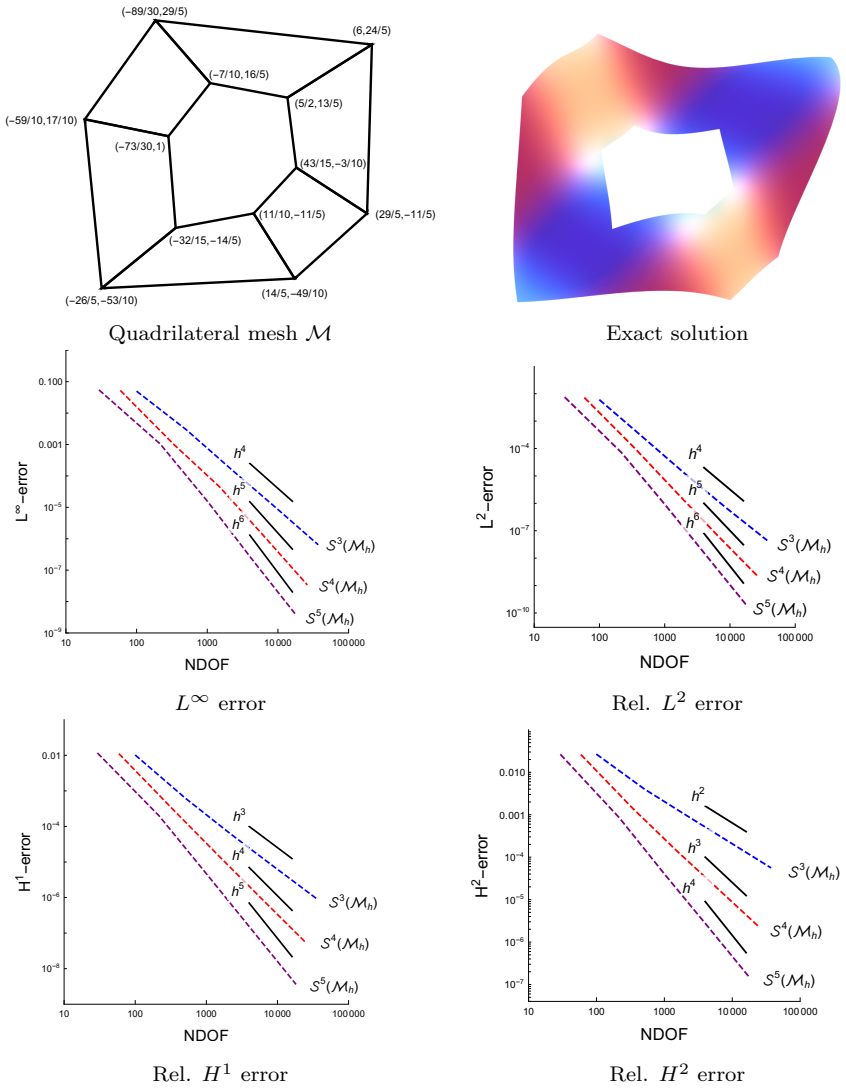

FIGURE 6. Solving the biharmonic equation (7.1) on the given quadrilateral mesh $\mathcal{M}$ (top row, left) for the exact solution (7.2) (top row, right) with the resulting L^∞ and relative L^2, H^1, H^2-errors (middle and bottom row). See Example 7.1.

(middle and bottom row) with respect to the number of degrees of freedom (NDOF), indicate for all considered degrees $p = 3, 4, 5$ and for both spaces $\mathcal{S}^p(\mathcal{M}_h)$ and $\mathcal{A}_h$ convergence rates of optimal order of $\mathcal{O}(h^{p+1})$, $\mathcal{O}(h^{p+1})$, $\mathcal{O}(h^p)$ and $\mathcal{O}(h^{p-1})$, respectively. While the spaces $\mathcal{S}^p(\mathcal{M}_h)$ perform slightly better than the spaces $\mathcal{A}_h$ for the case $p = 3$, it is in the opposite way around for the case $p = 5$. This is not really surprising, since for the case $p = 3$, the resulting spaces $\mathcal{S}^p(\mathcal{M}_h)$ are C^2 at all vertices $v \in \mathcal{V}_h$, while the spaces $\mathcal{A}_h$ are in general just C^1 at the vertices $v \in \mathcal{V}_h \setminus \mathcal{V}$,

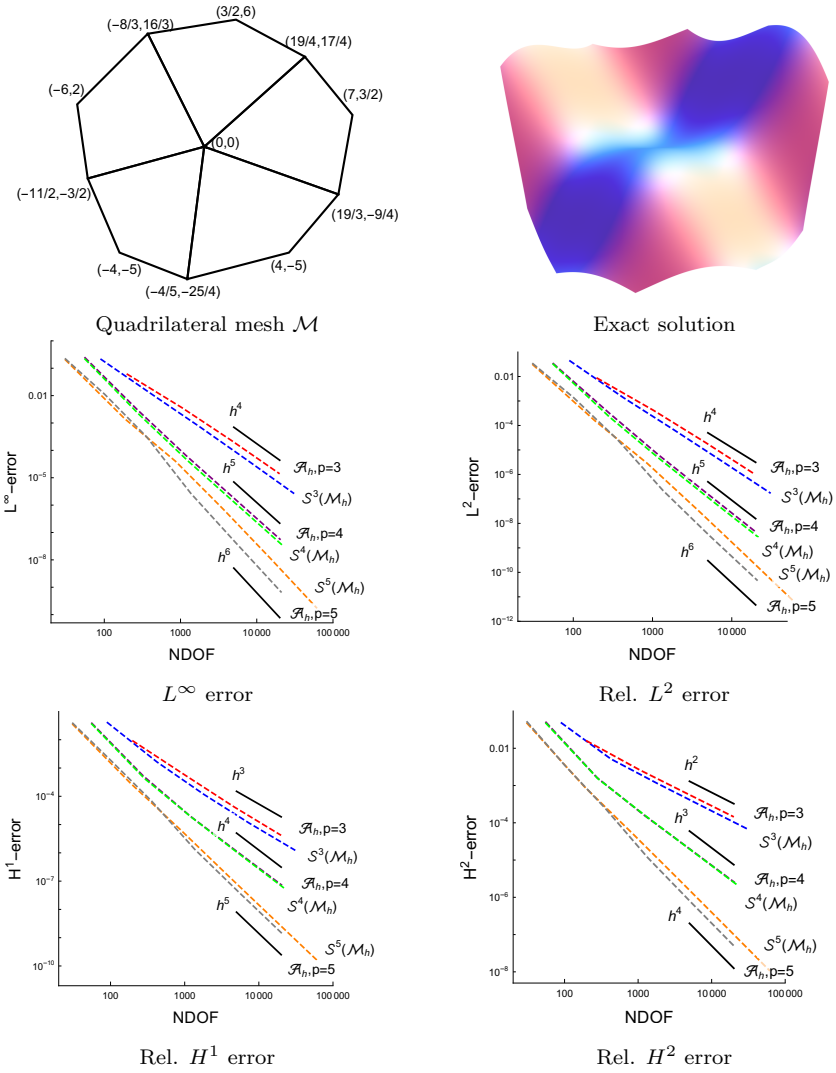

FIGURE 7. Solving the biharmonic equation (7.1) on the given quadrilateral mesh $\mathcal{M}$ (top row, left) for the exact solution (7.3) using the two C^1-smooth spaces $\mathcal{S}^p(\mathcal{M}_h)$ and $\mathcal{A}_h$ with the resulting L^∞ and relative L^2, H^1, H^2-errors (middle and bottom row). See Example 7.2.

and since for the case $p = 5$, e.g., the spaces $\mathcal{A}_h$ are C^3 at all edges $\varepsilon \in \mathcal{E}_h$, while the spaces $\mathcal{S}^p(\mathcal{M}_h)$ are in general just C^1 there.

Example 7.3. The goal is to compare the Brenner-Sung quadrilateral with the Argyris triangle of degree $p = 5$, comparing the spaces $\mathcal{S}^5(\mathcal{M}_h)$ and $\mathcal{S}^5(\mathcal{T}_h)$, respectively, where $\mathcal{T}_h$ is the resulting refined triangular mesh obtained via splitting each triangle in a regular way into four sub-triangles. For this, we solve the biharmonic equation (7.1) on two different computational domains, where the corresponding

quadrilateral and triangular meshes are given in the top rows of Fig. 8 and 9. In our examples, the quadrilateral and triangular meshes possess in each case the same vertices. The considered exact solution is on the one hand

$$u(x_1, x_2) = 200(x_1 x_2 (1 - x_1)(1 - x_2))^2 \tag{7.4}$$

for the computational domain from Fig. 8 (top row, right), and on the other hand

$$\begin{aligned} u(x_1, x_2) = \quad & \tfrac{1}{10^7} \left(\left(\tfrac{13}{5} - x_2 \right) \left(\tfrac{26}{5} + \tfrac{26 x_1}{15} - x_2 \right) \left(\tfrac{26}{5} + \tfrac{26 x_1}{15} + x_2 \right) \right. \\ & \left. \left(\tfrac{13}{5} + x_2 \right) \left(\tfrac{26}{5} - \tfrac{26 x_1}{15} + x_2 \right) \left(\tfrac{26}{5} - \tfrac{26 x_1}{15} - x_2 \right) \right)^2 . \end{aligned} \tag{7.5}$$

for the computational domain from Fig. 9 (top row, right), and fulfills for both cases homogenous boundary conditions of order 1. While in Fig. 8 the more regular configuration is used for the quadrilateral mesh compared to the triangular one, it is in the opposite way around for the meshes in Fig. 9. The numerical results, which are shown in the middle and bottom rows of Fig. 8 and Fig. 9, and which are compared with respect to the number of degrees of freedom (NDOF), indicate that the Brenner-Sung quadrilateral spaces $\mathcal{S}^5(\mathcal{M}_h)$ perform significantly better than the Argyris triangle spaces $\mathcal{S}^5(\mathcal{T}_h)$ for the more "quad-regular" case (cf. Fig. 8) and just slightly worse for the more "triangle-regular" case (cf. Fig. 9). However, the rates are not affected, as in all considered instances, the resulting L^∞-error as well as the relative L^2, H^1 and H^2-errors decrease with optimal order of $\mathcal{O}(h^6)$, $\mathcal{O}(h^6)$, $\mathcal{O}(h^5)$ and $\mathcal{O}(h^4)$, respectively.

8. Conclusion

We have described the construction of a novel family of C^1 quadrilateral finite elements, extending the Brenner-Sung quadrilateral construction from [8], possessing similar degrees of freedom as the classical Argyris triangle [1]. The presented method allows the simple design of polynomial as well as of spline elements. Amongst others, we have introduced a simple and local basis for the C^1 quadrilateral space, and have stated for particular cases explicit formulas for the Bézier or spline coefficients of the basis functions. We have also studied several properties of the C^1 quadrilateral space such as the optimal approximation properties of the space. Furthermore, the C^1 quadrilateral spaces are perfectly suited for solving fourth order PDEs, which has been demonstrated on the basis of several numerical examples solving the biharmonic equation on different quadrilateral meshes.

Since the classical Argyris triangle space and the Brenner-Sung quadrilateral space (and variants) presented here possess similar degrees of freedom, we are currently working on an approach to combine the C^1 triangle and quadrilateral element to construct a C^1 element for a mixed triangle and quadrilateral mesh. Further topics which are worth to study are e.g. the use of the C^1 quadrilateral elements for solving other fourth order PDEs such as the Kirchhoff plate problem, the Navier-Stokes-Korteweg equation, problems of strain gradient elasticity, and the Cahn-Hilliard equation, or the extension of our approach to quadrilateral meshes with curved boundaries.

Acknowledgments

The research of G. Sangalli is partially supported by the European Research Council through the FP7 Ideas Consolidator Grant *HIGEOM* n.616563, and by the Italian Ministry of Education, University and Research (MIUR) through the

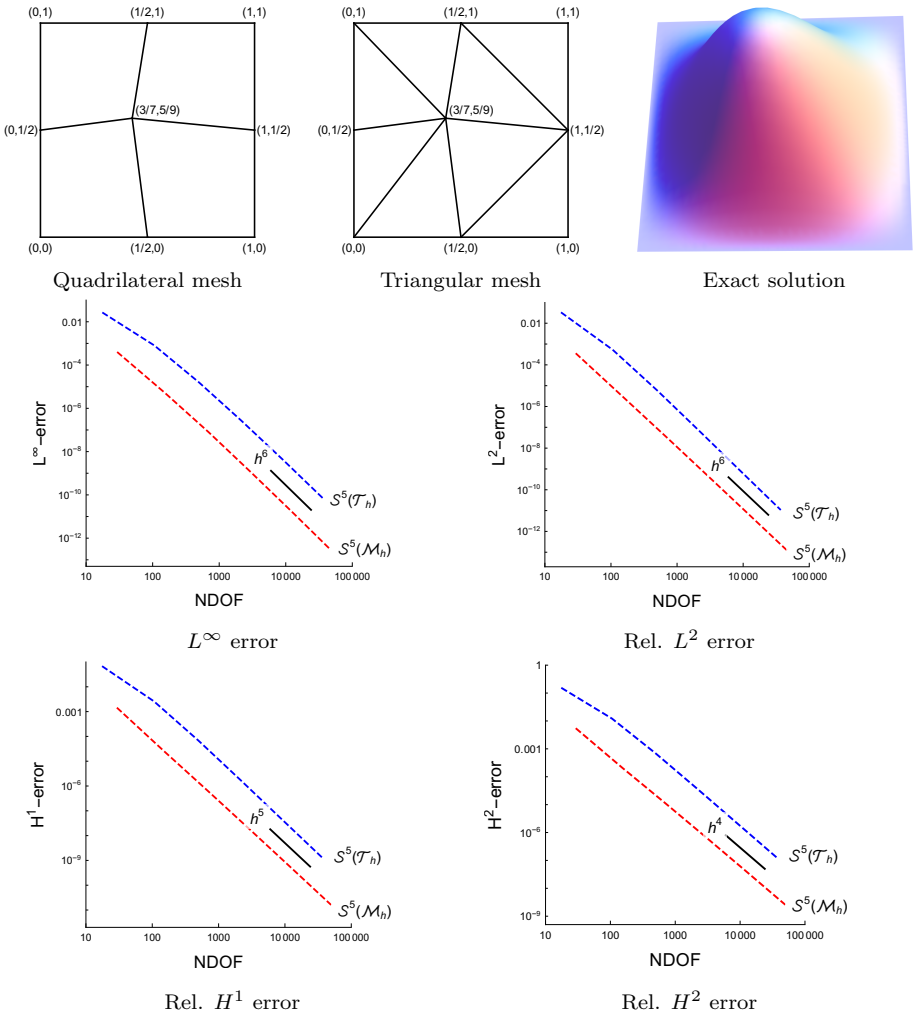

FIGURE 8. Comparison of using the Brenner-Sung quadrilateral spaces $\mathcal{S}^5(\mathcal{M}_h)$ with the Argyris triangle spaces $\mathcal{S}^5(\mathcal{T}_h)$ for solving the biharmonic equation (7.1) on the same computational domain defined either by a quadrilateral (top row, left) or a triangle mesh (top row, middle). Exact solution (7.4) (top row, right) and the resulting L^∞ and relative L^2, H^1, H^2-errors (middle and bottom row). See Example 7.3.

"Dipartimenti di Eccellenza Program (2018-2022) - Dept. of Mathematics, University of Pavia". The research of M. Kapl is partially supported by the Austrian Science Fund (FWF) through the project P 33023. The research of T. Takacs is partially supported by the Austrian Science Fund (FWF) and the government of Upper Austria through the project P 30926-NBL. This support is gratefully acknowledged.

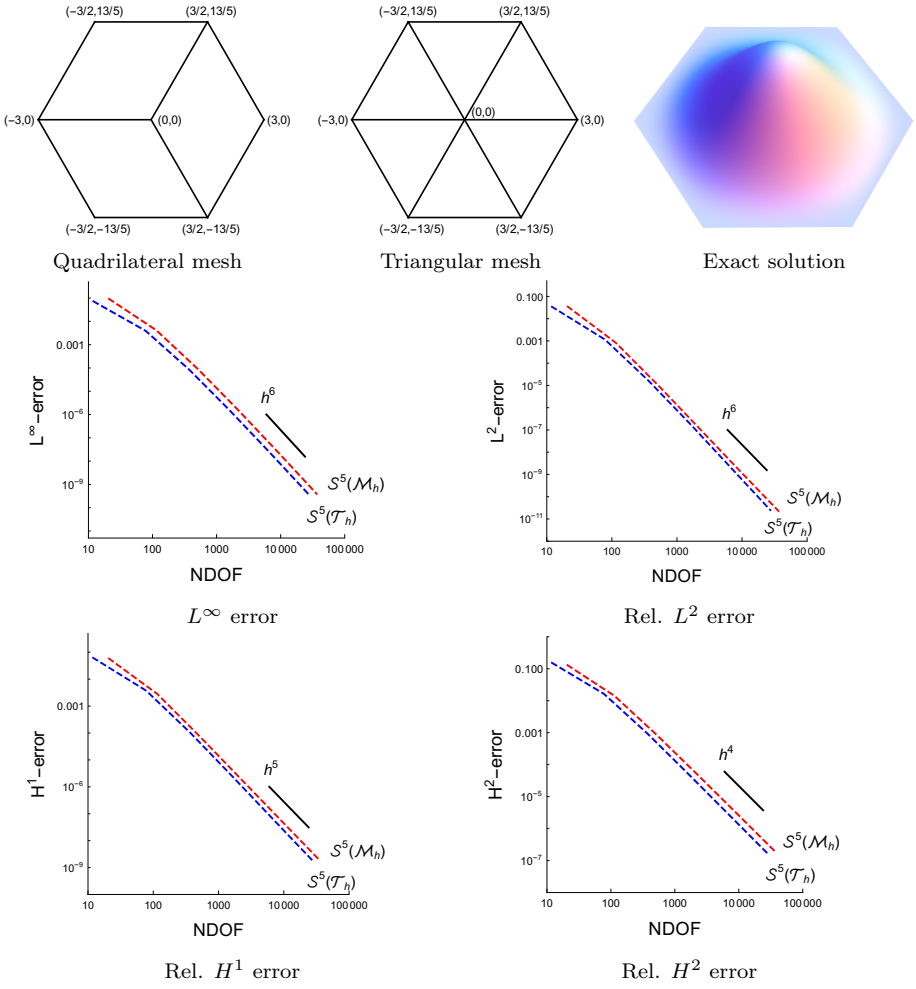

FIGURE 9. Comparison of using the Brenner-Sung quadrilateral spaces $\mathcal{S}^5(\mathcal{M}_h)$ with the Argyris triangle spaces $\mathcal{S}^5(\mathcal{T}_h)$ for solving the biharmonic equation (7.1) on the same computational domain defined either by a quadrilateral (top row, left) or a triangle mesh (top row, middle). Exact solution (7.5) (top row, right) and the resulting L^∞ and relative L^2, H^1, H^2-errors (middle and bottom row). See Example 7.3.

REFERENCES

1. J. H. Argyris, I. Fried, and D. W. Scharpf. The TUBA family of plate elements for the matrix displacement method. *The Aeronautical Journal*, 72(692):701–709, 1968.
2. L. Beirão da Veiga, A. Buffa, G. Sangalli, and R. Vázquez. Mathematical analysis of variational isogeometric methods. *Acta Numerica*, 23:157–287, 5 2014.
3. K. Bell. A refined triangular plate bending finite element. *International Journal for Numerical Methods in Engineering*, 1(1):101–122, 1969.
4. M. Bercovier and T. Matskewich. *Smooth Bézier Surfaces over Unstructured Quadrilateral Meshes*. Lecture Notes of the Unione Matematica Italiana, Springer, 2017.

5. A. Blidia, B. Mourrain, and N. Villamizar. G^1-smooth splines on quad meshes with 4-split macro-patch elements. *Computer Aided Geometric Design*, 52–53:106–125, 2017.
6. F. K. Bogner, R. L. Fox, and L. A. Schmit. The generation of interelement compatible stiffness and mass matrices by the use of interpolation formulae. In *Proc. Conf. Matrix Methods in Struct. Mech., AirForce Inst. of Tech., Wright Patterson AF Base, Ohio*, 1965.
7. S. C. Brenner and R. Scott. *The Mathematical Theory of Finite Element Methods*, volume 15. Springer Science & Business Media, 2007.
8. S. C. Brenner and L.-Y. Sung. C^0 interior penalty methods for fourth order elliptic boundary value problems on polygonal domains. *Journal of Scientific Computing*, 22(1-3):83–118, 2005.
9. F. Buchegger, B. Jüttler, and A. Mantzaflaris. Adaptively refined multi-patch B-splines with enhanced smoothness. *Applied Mathematics and Computation*, 272:159 – 172, 2016.
10. C.L. Chan, C. Anitescu, and T. Rabczuk. Isogeometric analysis with strong multipatch C^1-coupling. *Computer Aided Geometric Design*, 62:294–310, 2018.
11. C.L. Chan, C. Anitescu, and T. Rabczuk. Strong multipatch C^1-coupling for isogeometric analysis on 2D and 3D domains. *Comput. Methods Appl. Mech. Engrg.*, 357:112599, 2019.
12. P. G. Ciarlet. *The Finite Element Method for Elliptic Problems*, volume 40. Siam, 2002.
13. A. Collin, G. Sangalli, and T. Takacs. Analysis-suitable G^1 multi-patch parametrizations for C^1 isogeometric spaces. *Computer Aided Geometric Design*, 47:93 – 113, 2016.
14. J. A. Cottrell, T.J.R. Hughes, and Y. Bazilevs. *Isogeometric Analysis: Toward Integration of CAD and FEA*. John Wiley & Sons, Chichester, England, 2009.
15. P. Fischer, M. Klassen, J. Mergheim, P. Steinmann, and R. Müller. Isogeometric analysis of 2D gradient elasticity. *Comput. Mech.*, 47(3):325–334, 2011.
16. H. Gómez, V. M Calo, Y. Bazilevs, and T. J.R. Hughes. Isogeometric analysis of the Cahn–Hilliard phase-field model. *Computer Methods in Applied Mechanics and Engineering*, 197(49):4333–4352, 2008.
17. H. Gómez, T. J.R. Hughes, X. Nogueira, and V. M. Calo. Isogeometric analysis of the isothermal Navier–Stokes–Korteweg equations. *Computer Methods in Applied Mechanics and Engineering*, 199(25):1828–1840, 2010.
18. J. A. Gregory and J. M. Mahn. Geometric continuity and convex combination patches. *Computer Aided Geometric Design*, 4(1-2):79–89, 1987.
19. D. Groisser and J. Peters. Matched G^k-constructions always yield C^k-continuous isogeometric elements. *Computer Aided Geometric Design*, 34:67 – 72, 2015.
20. S. Hahmann and G.-P. Bonneau. Triangular G^1 interpolation by 4-splitting domain triangles. *Computer Aided Geometric Design*, 17:731–757, 2000.
21. T. J. R. Hughes, J. A. Cottrell, and Y. Bazilevs. Isogeometric analysis: CAD, finite elements, NURBS, exact geometry and mesh refinement. *Computer Methods in Applied Mechanics and Engineering*, 194(39-41):4135–4195, 2005.
22. Bert Jüttler. The dual basis functions for the Bernstein polynomials. *Advances in Computational Mathematics*, 8(4):345–352, 1998.
23. M. Kapl, F. Buchegger, M. Bercovier, and B. Jüttler. Isogeometric analysis with geometrically continuous functions on planar multi-patch geometries. *Computer Methods in Applied Mechanics and Engineering*, 316:209 – 234, 2017.
24. M. Kapl, G. Sangalli, and T. Takacs. Dimension and basis construction for analysis-suitable G^1 two-patch parameterizations. *Computer Aided Geometric Design*, 52–53:75 – 89, 2017.
25. M. Kapl, G. Sangalli, and T. Takacs. Construction of analysis-suitable G^1 planar multi-patch parameterizations. *Computer-Aided Design*, 97:41 – 55, 2018.
26. M. Kapl, G. Sangalli, and T. Takacs. Isogeometric analysis with C^1 functions on unstructured quadrilateral meshes. *The SMAI journal of computational mathematics*, 5:67–86, 2019.
27. M. Kapl, G. Sangalli, and T. Takacs. An isogeometric C^1 subspace on unstructured multi-patch planar domains. *Computer Aided Geometric Design*, 69:55–75, 2019.
28. M. Kapl, V. Vitrih, B. Jüttler, and K. Birner. Isogeometric analysis with geometrically continuous functions on two-patch geometries. *Computers and Mathematics with Applications*, 70(7):1518 – 1538, 2015.
29. K. Karčiauskas, T. Nguyen, and J. Peters. Generalizing bicubic splines for modeling and IGA with irregular layout. *Computer-Aided Design*, 70:23–35, 2016.
30. K. Karčiauskas and J. Peters. Refinable G^1 functions on G^1 free-form surfaces. *Computer Aided Geometric Design*, 54:61–73, 2017.

31. K. Karčiauskas and J. Peters. Refinable bi-quartics for design and analysis. *Computer-Aided Design*, pages 204–214, 2018.
32. J. Kiendl, Y. Bazilevs, M.-C. Hsu, R. Wüchner, and K.-U. Bletzinger. The bending strip method for isogeometric analysis of Kirchhoff-Love shell structures comprised of multiple patches. *Computer Methods in Applied Mechanics and Engineering*, 199(35):2403–2416, 2010.
33. J. Kiendl, K.-U. Bletzinger, J. Linhard, and R. Wüchner. Isogeometric shell analysis with Kirchhoff-Love elements. *Computer Methods in Applied Mechanics and Engineering*, 198(49):3902–3914, 2009.
34. M.-J. Lai and L. L. Schumaker. *Spline Functions on Triangulations*. Cambridge University Press, 2007.
35. T. Matskewich. *Construction of C^1 surfaces by assembly of quadrilateral patches under arbitrary mesh topology*. PhD thesis, Hebrew University of Jerusalem, 2001.
36. B. Mourrain, R. Vidunas, and N. Villamizar. Dimension and bases for geometrically continuous splines on surfaces of arbitrary topology. *Computer Aided Geometric Design*, 45:108 – 133, 2016.
37. T. Nguyen, K. Karčiauskas, and J. Peters. C^1 finite elements on non-tensor-product 2d and 3d manifolds. *Applied Mathematics and Computation*, 272:148 – 158, 2016.
38. T. Nguyen and J. Peters. Refinable C^1 spline elements for irregular quad layout. *Computer Aided Geometric Design*, 43:123 – 130, 2016.
39. J. Niiranen, S. Khakalo, V. Balobanov, and A. H. Niemi. Variational formulation and isogeometric analysis for fourth-order boundary value problems of gradient-elastic bar and plane strain/stress problems. *Comput. Methods Appl. Mech. Engrg.*, 308:182–211, 2016.
40. J. Peters. Smooth mesh interpolation with cubic patches. *Computer-Aided Design*, 22(2):109 – 120, 1990.
41. J. Peters. Smooth interpolation of a mesh of curves. *Constructive Approximation*, 7(1):221–246, 1991.
42. J. Peters. Geometric continuity. In *Handbook of computer aided geometric design*, pages 193–227. North-Holland, Amsterdam, 2002.
43. H. Prautzsch, W. Boehm, and M. Paluszny. *Bézier and B-Spline Techniques*. Springer, New York, 2002.
44. U. Reif. Biquadratic G-spline surfaces. *Computer Aided Geometric Design*, 12(2):193–205, 1995.
45. G. Sangalli, T. Takacs, and R. Vázquez. Unstructured spline spaces for isogeometric analysis based on spline manifolds. *Computer Aided Geometric Design*, 47:61–82, 2016.
46. L. L. Schumaker. *Spline Functions: Basic Theory*. Cambridge University Press, Cambridge, 2007.
47. M.A. Scott, D.C. Thomas, and E.J. Evans. Isogeometric spline forests. *Comp. Methods Appl. Mech. Engrg.*, 269:222–264, 2014.
48. A. Tagliabue, L. Dedè, and A. Quarteroni. Isogeometric analysis and error estimates for high order partial differential equations in fluid dynamics. *Computers & Fluids*, 102:277 – 303, 2014.
49. D. Toshniwal, H. Speleers, and T. J. R. Hughes. Smooth cubic spline spaces on unstructured quadrilateral meshes with particular emphasis on extraordinary points: Geometric design and isogeometric analysis considerations. *Computer Methods in Applied Mechanics and Engineering*, 327:411–458, 2017.

Johann Radon Institute for Computational and Applied Mathematics, Austrian Academy of Sciences, Austria
E-mail address: mario.kapl@ricam.oeaw.ac.at

Dipartimento di Matematica "F. Casorati", Università degli Studi di Pavia, Italy; Istituto di Matematica Applicata e Tecnologie Informatiche "E. Magenes" (CNR), Italy
E-mail address: giancarlo.sangalli@unipv.it

Institute of Applied Geometry, Johannes Kepler University Linz, Austria
E-mail address: thomas.takacs@jku.at